"ROLE OF MRI IN CORELATION WITH MR SPECTROSCOPY IN THE EVALUATION OF RING ENHANCING LESIONS IN BRAIN"

BY

Dr. MOHIT RAMESHRAO LOHEY M.B.B.S.

Dissertation submitted to the
BLDE UNIVERSITY (DEEMED TO BE UNIVERSITY)
SHRI B.M.PATIL MEDICAL COLLEGE, HOSPITAL AND RESEARCH CENTRE VIJAYAPUR, KARNATAKA

In Partial fulfillment
Of the requirements for the degree of

DOCTOR OF MEDICINE

IN

RADIO-DIAGNOSIS

Under the guidance of

Dr. SATISH D. PATIL M.D.
ASSOCIATE PROFESSOR

DEPATMENT OF RADIODIAGNOSIS
B.L.D.E.DEEMED TO BE UNIVERSITY, SHRI B. M. PATIL MEDICAL COLLEGE & RESERCH CENTER,VIJAYAPUR. 586103

2020

DECLARATION BY THE CANDIDATE

I hereby declare that this dissertation/thesis entitled **ROLE OF MRI IN CORELATION WITH MR SPECTROSCOPY IN THE EVALUATION OF RING ENHANCING LESIONS IN BRAIN** is a bonafide and genuine research work carried out by me under the guidance of **Dr. SATISH D. PATIL M.D. ASSOCIATE PROFESSOR.**

Dr. Mohit Rameshrao Lohey

Place : Vijayapura

Date: 29/092020

CERTIFICATE BY THE GUIDE

This is to certify that this dissertation entitled **"ROLE OF MRI IN CORELATION WITH MR SPECTROSCOPY IN THE EVALUATION OF RING ENHANCING LESIONS IN BRAIN"** is a bonafide research work done by **Dr. MOHIT RAMESHRAO LOHEY**in partial fulfillment of the requirement for the degree of **M.D. (Radio-Diagnosis).**

Dr. SATISH D. PATIL
ASSOCIATE PROFESSOR
Department of Radio-Diagnosis

Place :Vijayapura
Date : 29-09-2020

ENDORSEMENT BY THE HOD, PRINCIPAL/HEAD OF THE INSTITUTION

This is to certify that the dissertation entitled "**ROLE OF MRI IN CORELATION WITH MR SPECTROSCOPY IN THE EVALUATION OF RING ENHANCING LESIONS IN BRAIN**" is a bonafide research work done by **Dr. MOHIT RAMESHRAO LOHEY** under the guidance of **Dr. SATISH D. PATIL M.D, ASSOCIATE PROFESSOR.**

Dr. RAMESH PATTANSHETTI
PROFESSOR and HOD
Department of Radiodiagnosis
Shri B. M. Patil Medical College,Hospital& Research Center, Vijayapur, Karnataka.

Place :Vijayapura
Date : 29/09/2020

Dr. ARAVIND PATIL
Principal
Shri B. M. Patil Medical College,Hospital& Research Center, Vijayapura, Karnataka.

Place :Vijayapura
Date :29-09-2020

COPYRIGHT

Declaration by the Candidate

I hereby declare that Shri B. M. Patil Medical College,Hospital& Research Center, Vijayapura, Karnataka shall have the rights to preserve, use and disseminate this dissertation/ thesis in print or electronic format for academic / research purpose.

Dr. MOHIT RAMESHRAO LOHEY

ACKNOWLEDGEMENT

It is most appropriate that I begin by expressing my undying gratitude to the **ALMIGHTY GOD** for giving me the strength both mentally and physically to completethistask.

It gives me an immense pleasure to express my deepest gratitude and sincere thanks to my teacher and guide **Dr. SATISH D. PATIL** M.D., **ASSOCIATE PROFESSOR**, Department of Radio-Diagnosis, Shri B. M. Patil Medical College, Hospital& Research Center, Vijayapura for his guidance, valuable advice, constant support and encouragement during the entire course of the study, which helped me to complete my dissertationwork.

I am indebted to **Dr. RAMESH PATTANSHETTI** M.D.,PROFESSOR and Head, **DR. M.M.PATIL,** D.M.R.D and **Dr. SHIVANAND V. PATIL,** M.D., Department of Radio-Diagnosis, Shri B. M. Patil Medical College, Hospital & Research Center, Vijayapura, for preparing me for this task, guiding me with his superb talent and professional expertise, showing great care and attention to details and without his supervision and guidance this dissertation would have been impossible.

My special thanks and gratitude to **Dr. VISHAL S. NIMBAL**D.N.B., **Dr. RAVIKUMAR** M.D, and **Dr. SURESH KANAMADI** M.D., for their timely suggestions and constant encouragement.

My sincere thanks to **Dr. ARAVIND PATIL**M.S., Principal, Shri B. M. Patil Medical College, Hospital& Research Center, Vijayapura for their constant help and inspiration.

I must give my sincere thanks to my **PARENTS** for their abundant love, endurance, support, innumerable sacrifices and unceasing encouragement that has moulded me into the person I am today.

I extend my sincere thanks to my Post-graduate and My seniors. My special thanks to all the technicians of Shri B. M. Patil Medical College, Hospital & Research Center, Vijayapura.

I would like to thank **Mr. Shivakumar,** Librarian and his colleagues for their help during the preparation of this dissertation. .

Lastly I express my appreciation to all my patients for their willingness and co - operation during the study.

Dr. MOHIT RAMESHRAO LOHEY

Place :Vijayapura
Date :29-09-2020

LIST OF ABBREVIATIONS USED

AA	Aminoacids
Ac	Acetate
ADC	Apparent Diffusion Coefficient
CB	Cerebellum
Cho	Choline
CISS	Constructive Interference in steady state.
CNS	Central Nervous System
Cr	Creatine
CSF	Cerebro spinal fluid
CT	Computer Tomography
DRESS	Depth resolved spectroscopy
DWI	Diffusion weighted imaging
F	Frontal
FID	Free Induction Decay
Glu	Glutamine
Hz	Hertz
IFI	Invasive Fungal Infection
ISIS	Image selected in–vivo spectroscopy
Lac	Lactate
Lip	Lipids
Mi	Myo–inositol
MRA	Magnetic Resonance Angiography
MRI	Magnetic Resonance Imaging
MT	Magnetisation Transfer
NAA	N AcetylAspartate
NCC	Neurocysticercosis
O	Occipital
P	Parietal

P31	Phosphorus 31
PMRS,1H MR	Proton MR Spectroscopy
ppm	Parts Per Million
PRESS	Point Resolved Spectroscopy
rNAA	Reduced NAA
REL	Ring Enhancing Lesion
RF	Radio Frequency
SNR	Signal to Noise Ratio
STEAM	Stimulated Echo Acquisition Mode
Suc	Succinate
SV	Single voxel
T	Temporal
TBM	TB Meningitis
TE	Time to Echo
TMA	trimethylamine

ABSTRACT

Background & Objectives

This study is conducted to evaluate characteristic imaging findings in various ring enhancing lesions and their characterization.

Objectives

- Differentiate neoplastic vs non neoplastic brain lesions using conventional and advanced MR imaging techniques.
- Characterization of various ring enhancing lesions with imaging findings.
- Establish a differential diagnosis of the various ring enhancing lesions on conventional MRI.
- The role of MR spectroscopy in various ring enhancing lesions of brain with a single voxel proton MR spectroscopy and multiple voxel proton MR spectroscopy.

Methods

Overall 32 patients including 20 males & 12 females were evaluated in this study conducted at Shri B. M. Patil Medical College, Hospital & Research Center, Vijayapura from Nov 2018 to April 2020 over a period of 1& ½ years . MRI along with MRS was performed using PHILIPS ACHIEVA 1.5T & GE SIGNA 1.5T in patients ranging from ages of 10 months to 76 years.

Results

Out of the 32 patients evaluated 12 cases were tuberculomas, 8 cases of high grade glioma, 4 metastasis, 4 were NCC, 3 abscesses and 1 case of lymphoma. Seizures are the commonest presenting complaint seen in 32 cases.

Interpretation & Conclusion

MRI with MRS appears to be the most sensitive modality for characterization of intracranial ring enhancing lesions (RELs). MRI with help of MRS shows characteristic imaging findings which helps in differentiating the various RELs. Also it plays a major role by suggesting the correct diagnosis based on characteristic imaging findings which helps in patient management.

Keywords

MRI; Computer tomography, MR Spectroscopy; Tuberculoma; Neurocysticercosis; Abscess; Glioma.

TABLE OF CONTENTS

SL. No.		PAGE No.
1	INTRODUCTION	16
2	OBJECTIVES	20
3	REVIEW OF LITERATURE	21
4	METHODOLOGY	57
5	RESULTS	59
6	DISCUSSION	77
7	CONCLUSION	84
8	SUMMARY	86
9	BIBLIOGRAPHY	87
	ANNEXURES ➢ MASTERCHART ➢ PROFORMA ➢ CONSENTFORM	 96,97 98 99

LIST OF TABLES

Table No.	Contents	Page No.
1	Causes of multiple ring enhancing lesions of the Brain	17
2	Differential diagnosis of multiple ring enhancing lesions of the brain according to the size of the lesions	19
3	Diagnostic criteria for Neurocysticercosis	38
4	Incidence of ring enhancing lesions	59
5	Age – wise distribution	60
6	Sex – wise distribution	61
7	Clinical symptoms	62
8	Location of side of the lesion	63
9	Male – Female incidence of ring enhancing lesions	64
10	Number of ring enhancing lesions	65
11	Size of ring enhancing lesions	66
12	Diffusion in ring enhancing lesions	67
13	Metabolite peaks on MR spectroscopy	68

LIST OF IMAGES

Figure No.	Contents	Page No.
1	Normal MRI brain	26,27
2	Normal MR Spectroscopy curve	30
3	Philips Achieva 1.5T	69
4	GE SIGNA 1.5T	69
5	SAGAR - Tuberculoma	70
6	MAHESH - Tuberculoma	70
7	SIDDARTH- ABSCESS	72
8	SAROJINI - NCC	73
9	SHANTABAI - Metastases	74
10	SHRISHAIL - High Grade Glioma (Primary brain tumor)	75
11	KASHIMALI – CNS Lymphoma	76

LIST OF GRAPHS

Graph No.	Contents	Page No.
1	Incidence of ring enhancing lesions	59
2	Age –wise distribution	60
3	Sex – wise distribution	61
4	Clinical symptoms	62
5	Location of side of the lesion	63
6	Male – Female incidence of ring enhancing lesions	64
7	Number of ring enhancing lesions	65
8	Size of ring enhancing lesions	66
9	Diffusion in ring enhancing lesions	67
10	Metabolite peaks on MR spectroscopy	68

INTRODUCTION

One of the most common neuroimaging abnormality encountered by radiologist are ring-enhancing lesions (RELs). With available imaging techniques such as computed tomography and magnetic resonance imaging these lesions can be detected. Various etiologies may present as cerebral multiple ring-enhancing lesions[1,2]. On plain computed tomography, these lesions appears as hypodense or isodense mass lesions. Post contrast these lesions show ring type or disk-like enhancement within the region of hypodensity / isodensity. The lesions are generally of variable size and are surrounded by a varying amount of non enhancing vasogenic peri-lesional edema. These ring-enhancing lesions are typically located at gray and white matter junction, but can be located in the sub-cortical area, deep in the brain parenchyma or even superficial[3].

MRI demonstrate better contrast resolution between gray and white matter, tumor, ischaemia, edema, MS plaques, infections like abscess and hemorrhage which help in early detection of disease. Contributing to this is its sensitivity and capability to directly image anywhere without reformatting.

MR Spectroscopy is the best available noninvasive tool for differentiating between brain abscesses or non-infectious lesions such as primary brain tumor / lymphoma or brain metastasis. By analyzing the presence and/or ratio of tissue metabolites such as NAA, creatine, choline, lactate and other amino acids on MRS which provides additional information about the probable extension of the lesion and nature.

With higher signal-to-noise ratio and spatial resolution these faster MRS applications, allows radiologist to detect functional metabolic changes and helps in knowing morphology, nature of the tumour and physiological changes in surrounding brain parenchyma. Studies have demonstrated that HMRS is useful in monitoring disease progression, treatment effects and has a prognostic implication.[4]

TABLE 1: CAUSES OF MULTIPLE RING ENHANCING LESION OF THE BRAIN

- BACTERIAL
  - Pyogenic abscess
  - Tuberculoma and Tuberculous Abscess
  - Mycobacterium avium- intracellulare infection
  - Syphilis
  - Listerosis
- FUNGAL
  - Nocardiosis
  - Actinomycosis
  - Rhodo–coccosis
  - Zygomycosis
  - Histoplasmosis
  - Coccidioidomycosis

- Aspergillosis
- Mucormycosis
- Paracoccidioidomycosis
- Cryptococcosis

- PARASITIC
  - Neurocysticercosis
  - Toxoplasmosis
  - Amoebic Brain Abscess
  - Echinococcosis
  - Cerebral Sparganosis
  - Chaga's Disease
- NEOPLASTIC
  - Metastases
  - Primary Brain Tumor
  - Primary CNS Lymphoma
- INFLAMMATORY ANDDEMYELINATING
  - Multiple Sclerosis
  - Acute Disseminated Encephalomyelitis
  - Sarcoidosis
  - Neuro – Behcet's disease
  - Whipple's Disease
  - Systemic Lupus Erythematous

TABLE 2: DIFFERENTIAL DIAGNOSIS OF MULTIPLE ENHANCING LESIONS OF THE BRAIN ACCORDING TO THE SIZE OF THE LESIONS

- MILIARY
  - Metastasis
  - Tuberculoma
- SMALL
  - Metastasis
  - Tuberculoma
  - Cysticercus Granuloma
  - Inflammatory Disorders of Brain (Vasculitis, Behcet Disease)
  - Sarcoidosis
- MEDIUM
  - Metastasis
  - Primary Brain Tumor
  - Tuberculoma
  - Fungal Granuloma
  - Toxoplasmosis
  - Sarcoidosis
  - Demyelinating Disorders
- LARGE
  - Cerebral Abscess
  - Tuberculous Abscess
  - Primary Brain Tumor
  - Fungal Abscess
  - Tumefactive Demyelinating Lesion

OBJECTIVES OF THE STUDY

- Differentiate neoplastic vs non neoplastic brain lesions using conventional and advanced MR imaging techniques.
- Characterization of various ring enhancing lesions with imaging findings.
- Establish a differential diagnosis of the various ring enhancing lesions on conventional MRI.
- The role of MR spectroscopy in various ring enhancing lesions of brain with a single voxel proton MR spectroscopy and multiple voxel proton MR spectroscopy.

REVIEW OF LITERATURE

EMBRYOLOGY

The central nervous system (CNS) appears at the beginning of the 3rdweek as a slipper-shaped plate of thickened ectoderm , the neural plate. This plate is located in the mid-dorsal region in front of the primitive pit. Its lateral edges soon become elevated to become the neural folds. These neural folds become more elevated, approach each other in the midline and finally fuse thus forming the neuraltube.

By the fourth week of gestation, three vesicular dilatations develop at the rostral portion of the neural tube, thereby defining the forebrain (prosencephalon), midbrain (mesencephalon) and hindbrain (rhombencephalon).

By the fifth week of gestation , the developing forebrain has divided into a cephalic telencephalon and a caudal diencephalon . The developing hindbrain has subdivided into a cephalic metencephalon and a caudal myelencephalon. The metencephalon later becomes the pons and cerebellum while the myelencephalon forms the medulla oblongata.

Bilateral diverticula from the telencephalic end of the neural tube form the cerebral hemispheres. These hemispheres undergo complex expansion and folding with formation of permanent primitive fissures by the fourth month. Three major flexures, the midbrain, pontine and cervical flexures divide the developing brain into the cerebrum, cerebellum and spinal cord.

Early in development the cerebral hemispheres are smooth – surfaced (lissencephalic), and a germinal matrix of primitive cells surrounds each lateral ventricle. Cells from the germinal matix proliferate, migrate outward to the cortex in an “inside out” sequence,and mature as neural and glial cells. The

germinal matrix forms at about 7 weeks gestational age and involutes at about 28 to 30 weeks , although it persists in the form of focal cell clusters upto weeks 36 through 39 . During the sixth and seventh fetal months, the cerebral surfaces convolute to form primitive gyri and sulci. Thus, the adult pattern can already be recognized towards the end of gestation. Concomitant with cortical development is the formation of fiber tracts, including the commissures between the two cerebralhemispheres.

NORMAL ANATOMY

Brain parenchyma, cranial nerves, meninges and CSF spaces form the contents of the cranial cavity. The anatomy of the head is studied in the form of cross sectional images. Axial, sagittal and coronal planes areobtained.

CEREBELLAR HEMISPHERES

The falx cerebri and inter-hemispheric fissure separates the two cerebral hemispheres. Each cerebral hemispheres consists of outer gray matter (cerebral cortex) and inner white matter. Sulci and Gyri are found on the surface of the cerebral hemispheres. Each hemisphere is divided into five lobes- frontal, parietal, temporal, occipital and insula (central lobe). The rolandic fissure (central fissure)starts from the superior mid hemisphere and extends anteriorly and inferiorly to separate the frontal lobe from the parietal lobe. On the lateral surface the sylvian fissure begins anteriorly and inferiorly, separating the frontal lobe from the temporal lobe.

Corpus callosum is a band of central white matter that connects two cerebral hemispheres. The parts of the corpus callosum are the genu, body, splenium and

rostrum. Basal ganglia represent the central gray matter. It consists of caudate nucleus, lentiform (globus pallidus and putamen) nucleus, claustrum and amygdala. The internal capsule is a boomerang shaped thick white matter, consisting of anterior limb, genu and posterior limb. It is bounded laterally by lentiform nucleus, anteriomedially by caudate nucleus and posteromedially by thalamus. The centrum semiovale constitutes the white matter of the cerebralhemispheres.

The diencephalon is made up of thalami, geniculate bodies (medial and lateral), epithalamus, subthalamus and hypothalamus.

BRAIN STEM

Brain stem is formed by the midbrain, pons and medulla oblongata. Midbrain is the superior part of brain stem, which forms the connecting link between the forebrain and hind brain. It consists of the larger ventral portion called cerebellar peduncle and a smaller dorsal portion calledtectum.

The triangular spacebetween the two cerebral peduncles form the interpeduncular fossa or cistern. The tectum is composed of four rounded projections called colliculi or corpora quadrigemina. The pons connects with the midbrain above and medulla below. It has an anterior bulge, which is caused by the middle cerebellar peduncles and pontocerebellar connections. The pons is separated from the medulla by the inferior pontine sulcus, and from the cerebral peduncles by superior pontine sulcus. The medulla is the caudal most portion of the brain stem and connect to the cervical cord. At the level of foramen magnum it contains anterior median fissure and posterior median sulcus.

CEREBELLUM

Cerebellum occupies the greater part of posterior cranial fossa. It is situated postero-lateral to the pons and medulla and is separated from these two structures by the fourth ventricle. The cerebellum consists of two hemispheres, which are connected in the midline by vermis. Three peduncles superior, middle and inferior attach it to the brainstem, which are connected to midbrain, pons and medulla respectively.

CSF SPACES

The ventricular system within the brain parenchyma and subarachnoid cisterns and sulci surrounding the brain compress the CSF spaces. The CSF is mainly produced by the choroid plexus situated in the lateral ventricles. The ventricles of the brain are lateral ventricles, third ventricle and fourth ventricle. The two lateral ventricles communicate through the foramen of Munro with the third ventricle. The third ventricle is connected to the fourth ventricle by cerebral aqueduct (aqueduct of sylvius). The fourth ventricle in turn is continuous with the narrow central canal of spinal cord and through foramen of Magendie and Luschka into the subarachnoid cisterns.

CRANIAL NERVES

There are twelve pairs of cranial nerves. With MRI, it is possible to identify the cisternal segment of the cranial nerves.

VASCULAR SYSTEMS

The two internal carotid and two vertebral arteries supply brain. These four arteries lie within the subarachnoid space, and their branches anastomose on the inferior surface of brain to form the circle of Willis. The anterior communicating, anterior cerebral, internal carotid, posterior communicating, posterior cerebral and basilar arteries contributes to the formation of the circle.

The circle of Willis allows the blood that enters by either internal carotid or vertebral arteries to be distributed to any part of both cerebral hemispheres. The cerebral venous system is composed of dural sinuses, superficial cortical and deep (medullary and subependymal) veins.

DURA AND DURAL STRUCTURES

The meninges – piamater, arachnoid membrane and duramater cover the brain. The piamater follows all the gyri and is separated from the arachnoid membrane by CSF. The duramater is separated from the arachnoid membrane by a potential subdural space. The outer layer of the dura is attached to the periosteum of the bony calvarium. The inner layer of the dura forms folds within the cranial vault. The two major folds are falx cerebri and tentorium cerebelli. The falx cerebri separates the two cerebral hemispheres and tentorium cerebelli separates the superior surface of the cerebellum from the inferior surface of the cerebral hemispheres.

IMAGE 1: NORMAL MRI BRAIN

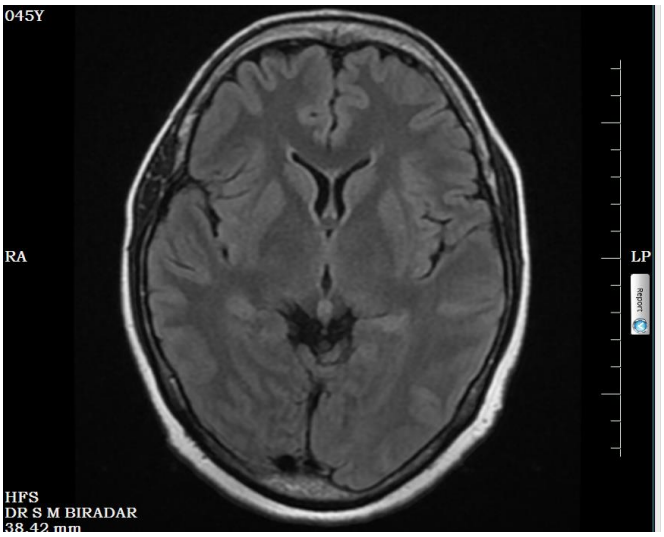

FLAIR Axial

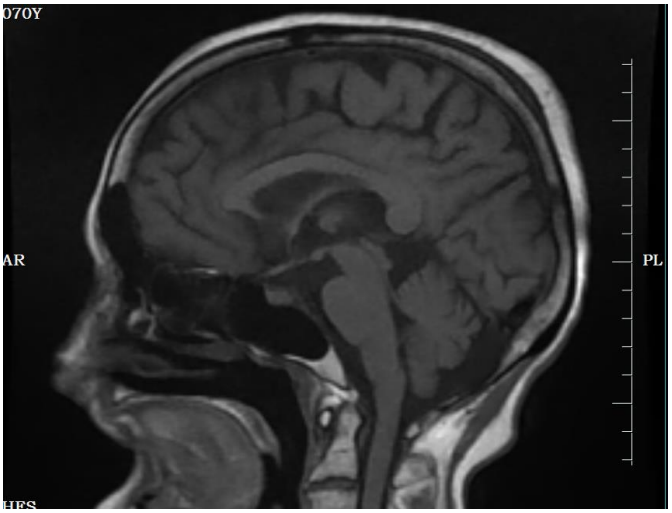

T1 sagittal

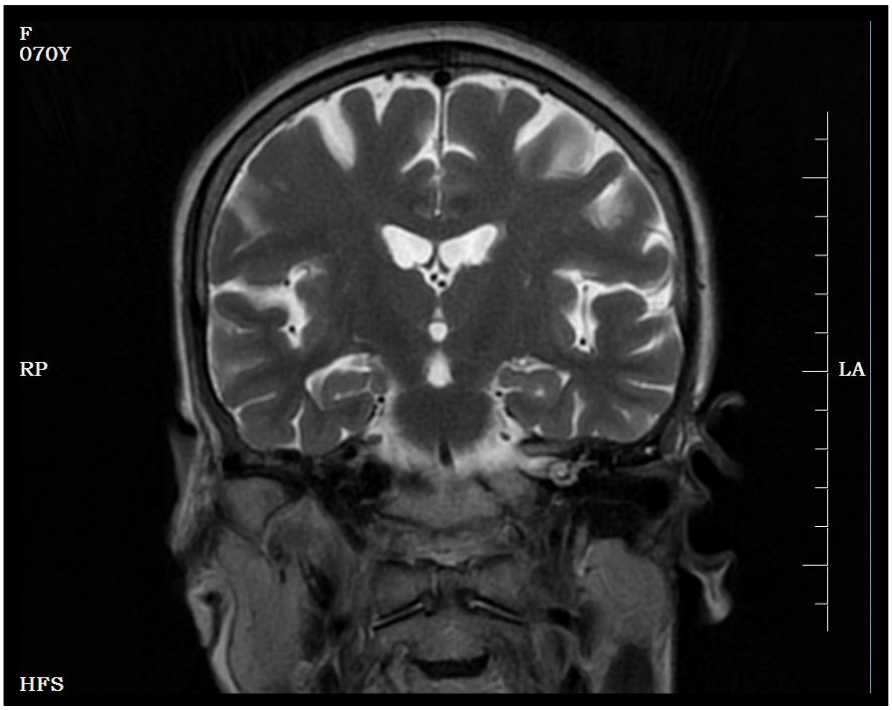

T2 Coronal

Images showing normal MRI anatomy of the brain

MAGNETIC RESONANCE SPECTROSCOPY

MRS measures absolute and relative levels of various brain tissue metabolites and is a non-invasive physiological imaging of the brain. MRS differs from conventional MRI only by manner in which the data are processed and presented. The data is collected in the time domain of free induction decay signal to obtain information about the nuclear relaxation time namely T1 and T2, which is processed to generate an anatomic image in convectional MRI. However in MRS time domain information is converted to frequency domain information via Fourier transformation of the free induction decay time domain signal.

MRS receives a sum of individual metabolite signal amplitudes vs time in response to radiofrequency excitation i.e similar to MR imaging. It presents with the individual information as metabolite peak amplitude vs frequency, where frequency can be expressed in absolute values of Hertz or relative units of parts per million. Its relative amount and chemical structure determine the amplitude and frequency of a particular metabolite peak. The relative resonance frequency position of each peak on the plot is dependent on the chemical environment of that nucleus and determines subtle chemical shifts in their absolute (Hz) or relative (ppm) resonance frequencies. An advantage of the ppm scale is that it allows relative chemical shifts to be expressed independently of the main magnetic field strength that is used. As spectral resolution improves, chemical shifts narrow into singlets or split into doublets, triplets, and other multiplets because of a phenomenon known as spin –spin coupling or j coupling. J coupling is responsible for splitting the lactate peak into a doublet in the proton spectrum.

In 1995 Food and Drug Administration (FDA) approved the use of fully automated MR spectroscopic sequences for clinical use in neuro-radiology.

Normal brain metabolites

CHEMICAL COMPOUND	CHEMICAL SHIFT	COMMENTS
N-Acetylaspartate (NAA)	2.0	Neuronal marker.
Creatine/phosphocreatine	3.0,3.9	Energy metabolism. Supplier of phosphate to convert ADP to ATP.
Choline (cho)	3.2	Cell membrane marker.
Myo–inositol (ml)	3.6	Glial cell marker, osmolyte hormone receptor mechanisms
Glutamate(glu) Glutamine (Gln) (Glu+Gln=Glx)	2.1-2.5	An excitatory neuro transmitter and regulator
Lipids (lip)	0.9-1.4	Cell break down/ brain destruction indicator.
Lactate (Lac)	1.3	An end product of anaerobic glycolysis

Image 2: Normal Single Voxel MR Spectrum

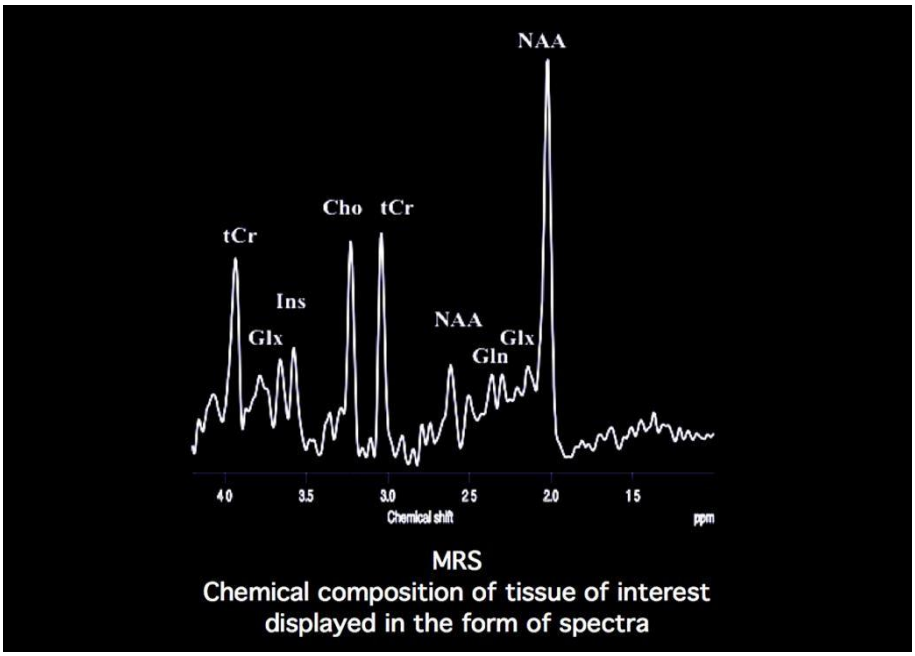

A normal MR spectrum is read from viewers right to left with metabolite peaks at various locations on x axis, starting from lipids at 0.9 and 1.3ppm, lactate at 1.3ppm, (as a doublet), N- acetylaspartate (NAA) at 2.0ppm, creatine (Cr) at 3.0ppm and choline (Cho) at 3.2ppm and Myo-inositol (mI) at

3.6ppm. A line joining mI, Cr, Cho and NAA forms 45-degree angle to x axis when they are present in normal proportions which is called as Hunters angle. Hunters angle changes as we shift from short to long echo time (TE) changing repetition time (TR) and change in location of voxel from cortex tomidbrain.

Metabolites in proton spectra and their significance:

Lipids

Lipids are broad peaks that occur at 0.9 and 1.2 parts per million (ppm). In normal spectrum lipid peak is obscured as very little lipid is noted in healthy tissues. The presence of lipid can be seen in tuberculous granulomas

and brain tumours where in lipid indicates necrosis.

Lactate

Lactate is generally seen as a doublet (two peaks close together) that has a frequency of 1.33ppm. Healthy tissue does not have sufficient lactate to be detectable with MRS. lactate is a product of anaerobic glycolysis detected in diseased brain, which is oxygen starved like in stroke, mitochondrial myopathy, encephalopathy, lactic acidosis, recovery from cardiac arrest and neonatal hypoxia, etc. It is of greatest diagnostic value in cases of brain injury or trauma where hypoxia is part of the differential. It is also a nonspecific marker of tumor aggressiveness and is found in cysts and abscesses of all types. Lactate levels may be elevated secondary to inflammatory cellinfiltrates.

Choline

Choline or trimethylamine (TMA) is a term for several soluble components of brain myelin and fluid – cell membranes. Choline resonates at 3.2ppm. As most choline-containing brain constituents are not normally soluble, pathological alterations in membrane turnover (tumour, leukodystrophy, multiple sclerosis) result in a massive increase in MRS-visible Cho. Choline increases in active demyelinating lesions because membrane phospholipids are released during active myelin breakdown. Many brain tumours are also associated with their increased cellular density and compression of surrounding brain tissue. Infants with active myelination occurring also have increased levels of Cho and mI on MRS, as compared toadults.

Creatine

Creatine (Cr) is often used as an internal standard to which the resonance intensities of other metabolites are normalised. The primary resonance of creatine lies at 3.0ppm. As phosphocreatine, it is the central energy marker of both neurons and astrocytes. Focal decrease of Cr signals is noted in acute destructive pathologies like malignant tumors. Spectroscopic imaging allows these focal decreases in Cr to be visualized and provide the option of normalizing the contralateral homologous region in situation where this is normal.

N- Acetylaspartate (NAA):

N-Acetylaspartate is noted at 2.0ppm. NAA is an amino acid derivative synthesized in neurons and transported down the axons. It is therefore a most specific marker of viable neurons, axons and dendrites. The diagnostic value of NAA lies in the ability to quantify neuronal injury or loss on a regional basis. NAA can be used as a surrogate marker of neuronal integrity. NAA can be detected in the cerebral cortex and white matter of fetuses as early as 16 weeks gestation. Levels of NAA/Cr increase rapidly during the first few years of life, after this levels increase less than 1% a year until reaching adult values by 16 years of age.

Decreases in the relative NAA concentrations are observed in pathologies well known to involve neuronal loss or damage, e.g., degenerative disorders, multiple sclerosis and stroke. The ability to quantify neuronal loss or damage in vivo is one of the most important potential applications of MRS in cerebral disorders.

Myo- inositol (mI)

Myo-inositol is a polyol (a sugar like molecules) that resonates at 3.6ppm. Myo-inositol is an osmolyte for brain volume regulation. It is mostly a diagnostic modifier in those diseases that affect Cho (tumor, multiple sclerosis, etc) As an astrocyte marker and osmolyte , mI contributes specificity in dementia diagnosis and adds specificity to monitoring hepatic encephalopathy and hyponatremic brain syndromes.

Glutamate-glutamine (Glx)

A mixture of closely related amino acids and amines. They are closely involved in excitatory and inhibitory neurotransmission that lies between 2.1 and 2.4 ppm. As these are integral products of intact kreb cycle activity and mitochondrial redox systems, Glx offers a vital marker(s) in MRS of stroke, lymphoma, hypoxia and many metabolic braindisorders.

Water and fat suppression:

As water and fat in the tissues are present at thousands of times greater concentrations than the metabolites, they consequently produce signals that are thousands of times greater. This causes difficulty in recording the tiny signals from the metabolites. It is therefore necessary, in either suppress the excessively large signals from water and fat or avoid exciting them in the first place.

Water and fat suppression includes saturating the water or fat resonance selectively by inverting the magnetization of the water or fat and acquiring the spectrum when the magnetization from them is zero. Unlike lipids within the

skull and scalp, lipids inside the brain normally do not cause a problem as they are relatively immobilized in membranes and produce signals with very short T2s that die away before the spectra are acquired. Intracerebral lipids can become visible under certain pathological circumstances.

NEUROCYSTICERCOSIS

Neurocysticercosis is the most common CNS parasitic infection of the human. The causative agent in cysticercosis is the pork tape worm- Taenia solium. Each cyst measures 3-18 mm in diameter and contains a scolex. When alive, the cyst provokes minimal surrounding inflammation and remains viable for 2-6 years after infestation. As the cyst dies antigen and metabolic products leak from the wall into the surrounding brain, inciting an intense inflammatory reaction in the adjacent parenchyma with edema and mass effect. The patient may become symptomatic with seizures or focal neurological signs. The clear cyst fluid becomes turbid and gelatinous. The cyst then collapses, degenerates and often calcifies.

The location of involvement can be meningo-basal, parenchymal, intraventricular or the combination of the sites.

Neurocysticercosis imaging findings are quite often characteristic. Imaging findings in each stage reflect underlying changes in the disease process and host response[5]. Parenchymal cysticercosis have been classified into following four stages.

Vesicular Stage

After several weeks the larva develops into a cyst containing the scolex. In 3-12 months, a cysticercusis fully grown and contains clear fluid. Mature cysts are readily apparent on CT and MR images and measure 5-20 mm. Gray-white matter junction are most common sites for cysts but are also seen in the basal ganglia, cerebellum and brainstem. Smooth thin walled cyst and a 2 to 4 mm scolex is identified within the cyst. Little or no edema surrounds the cyst.

CT shows a non-enhancing or mildly enhancing cyst wall containing a small scolex and CSF-density cystic fluid. A low-signal-intensity cyst cavity containing a nodule

that is isointense or hyperintense relative to white matter is seen on Tl-weighted MR images. On T2-weighted MR images the scolex can be isointense or hyperintense and can be obscured by high signal intensity cystic fluid. The scolex is better seen on proton density-weighted images.

Colloidal Vesicular Stage

In this stage the larva begins to degenerate. As the larva dies the scolex disintegrates and the host's inflammatory response causes a fibrous capsule to form with surrounding parenchymal edema. The severity of this inflammatory response varies widely because it depends on the host's immune response to cysticerci infestation.

A diffuse encephalitis may occur, especially in children and after use of the oral antihelmintic agents praziquantel or albendazole, requiring large doses of corticosteroids to control brain edema[6]. CT depicts ring-enhancing cystic lesions with hyperdense fluid content and surrounding edema. T1 –weighted MR images show a cyst hyperintense to CSF because of proteinaceous fluid and accumulated debris within the cystic cavity. T2- weighted MR images show a hyperintense cyst surrounded by hyperintense parenchymal edema[5.]

Granular Nodular Stage

In this stage, the cyst retracts and forms a granulomatous nodule that will later calcify. CT reveals an enhancing nodule with mild surrounding edema. MR images show a thick enhancing ring or nodule with or without surrounding edema simulating tuberculoma, granuloma, or metastatic nodule.

Nodular Calcified Stage

In this final stage, the granulomatous lesion is shrunken and completely calcified. On CT the lesion appears as single or multiple calcified nodules. These nodules are hypointense on all MR imaging sequences.

Cisternal Cysticercosis

In cisternal cysticercosis the subarachnoid spaces and adjacent meninges are involved. Cisternal cysticercosis and spinal cysticercosis are rare and are frequently associated with parenchymal cysticercosis. Cysts within the cistems may manifest as space-occupying lesions that may cause obstructive hydrocephalus. Hydrocephalus may also be caused by basilar arachnoiditis. Larvae can have a racemose form that occurs in the subarachnoid spaces and may simulate a low-density tumor in the sellar or cerebello-pontine angle region. The subarachnoid cysts usually lack a scolex.[7]

Intra-ventricular Cysticercosis

Intraventricular cysticercosis often leads to obstructive hydrocephalus and ventriculitis[8]. On MR imaging, the scolex, subependymal reaction, and cyst wall are readily apparent, indicating the intraventricular larva.

A combination of elevated levels of lactate, alanine, succinate and choline and reduced levels of NAA and creatine are common MRS findings in neuro-cysticercosis. [9]

Identification of the scolex is essential for making a definitive diagnosis of neurocysticercosis (NCC). This scolex may be missed on routine sequences but a 3D sequence like CISS will demonstrate it. The cyst wall and scolex are well visualized on CISS. The increased sensitivity of the CISS sequence is due to its higher contrast to noise ratio and may also be related to accentuation of the T2 value between the cystic fluid and the surrounding CSF.

TABLE 3: MODIFIED DIAGNOSTIC CRITERIA FOR NEUROCYSTICERCOSIS

- ABSOLUTE
  - Demonstration of the parasite histologically.
  - Multiple cystic lesions with or without the scolex.
- MAJOR
  - Lesion highly suggestive of neurocysticercosis on imaging
  - Positive serum EITB assay.
  - Resolution of intracranial cystic lesion following albendazole and praziquantel
  - Spontaneous resolution of small single ring enhancing lesion.
- DIAGNOSIS WITH CAUTION
  - In old patient.
  - RVD patients.
  - Patients known case of tuberculosis or malignancy.
  - Patients with grossly abnormal neurological examination.

- DEFINITIVE
  - One absolute criterion.
  - Two major and one minor criteria.
- PROBABLE
  - One major plus two minor criteria.
  - Three minor criteria.

ABSCESS

Pyogenic brain abscesses are often multiple. Cause of the spread to brain is by hematogenous spread of bacteria and are commony found in the MCA (middle cerebral artery) territory. Cyanotic heart disease, endocarditis, suppurative lung diseases, skin infection and abdominal and pelvic infections are the primary infection sources in patients with multiple brain abscesses. They are common in the patients with diabetes, congenital cardiac defects or prosthetic cardiac valves, intravenous drug abusers, human immunodeficiency virus infection, organ transplant recipients, and patients on chemotherapy.

STAGES OF ABSCESS FORMATION

EARLY (3-5 days) AND LATE (5-14 days) CEREBRITIS STAGE

They are differentiated on the basis of mass effect present in the latter. On T1-weighted images, cerebritis may be visible as an ill-defined, iso-intense to hypointense area relative to adjacent normal brain parenchyma. On FLAIR and T2-weighted images, early cerebritis demonstrates as an area of increased signal intensity with mass effect[10]. Cerebritis shows patchy restricted diffusion on DWI.

EARLY (2-4weeks) AND LATE (weeks to months) CAPSULAR STAGE

They are differentiated on the basis of peripheral edema which is present in the former and absent in the latter stage. A typical abscess with central hypointense necrosis or a cavity is slightly hyperintense to CSF, the surrounding edematous brain parenchyma is mildly hypointense to normal brain parenchyma on T1WI. The mature and surgically drainable abscess commonly has a rim with distinctive features[11].

The rim is isointense to mildly hyperintense to white matter on T1WI and is hypointense on T2WI. The absolute thing that is necessary post contrast (gadolinium) in a abscess is smooth ring enhancement of capsule. The abscess ring is most commonly very smooth, regular in thickness, and thin walled (approximately 5 mm in thickness), although it may be thinner along its medial margin, possibly due to variations in perfusion of gray and white matter. Only infrequently, nodular or solid enhancement, incomplete thin rings or thick and irregular rings may be observed and these should make the radiologist consider other diagnoses.

Abscesses shows diffusion restriction on DWI, with a corresponding low on apparent diffusion coefficient (ADC) values[12,13]. This is directly related to the cellularity and viscosity of the pus contained within an abscesscavity[12]. Incontrast, high-grade gliomas and metastases with central necrosis have a low signal on DWI and high apparent diffusion coefficient values[12]. Restricted diffusion has also been described uncommonly in other ring-enhancing lesions. These lesions include metastases, rarely glioblastoma multiforme, and even residual diffusion change persisting into the early stages of enhancement of an evolving recent cerebral infarction.

The MR spectroscopy (MRS) pattern derived from the central portion of an abscess appears to be fairly characteristic. Multiple elevated amino acids with corresponding resonances such as acetate (1.92 ppm), lactate (1.3 ppm), alanine (1.5 ppm),

succinate (2.4 ppm), and pyruvate, as well as a complex peak at 0.9 ppm indicating amino acids valine, leucine, and isoleucine may be seen in an abscess.[13-18] Acetate, lactate, succinate and pyruvate are metabolic end products arising from microorganisms[15].

TUBERCULOMA

CNS tuberculosis have multiple varieties, including tubercular meningitis, abscess, focal cerebritis and tuberculoma. They can be single or multiple and can be seen at any location in the brain parenchyma. The number of identified lesions per patient may range from one to 12 (or more), with the size varying from 1 mm to 8 cm. Its presence in the ventricular system is very rare. Although no precise patterns of localization have been observed according to race, age, or sex, children develop infratentorial tuberculomas more commonly than do adults. Symptoms are often limited to seizures and mass effect, resulting in an increased intracranial pressure. Neurological deficit reflects the topographic location of the lesion. These lesions originate as a conglomerate of microgranuloma in an area of tuberculous cerebritis that join to form a non-caseating tuberculoma. In most cases, subsequent central caseous necrosis develops that is initially solid, but in some instances, may eventually liquefy.

Intracranial tuberculomas usually show hypo- or isointensity or central hyperintensity with a hypointense rim on T2WI and isointensity and/or hypointensity on T1WI.[19] Certain tuberculomas show a varied range of signal intensities on MRI. Depending on its stage of maturation, a tuberculoma's appearance varies on MRI, i.e., whether noncaseating, caseating with a solid center, or caseating with a liquid center.[19,20] A noncaseating tuberculoma appears hyperintense on T2WI and slightly hypointense on T1WI.[19] These granulomas show homogenous enhancement after injection of paramagnetic contrast on T1WI. A solid caseating tuberculoma appears relatively iso- to hypointense on both T1WI and T2WI with an iso- to hyperintense rim on T2WI. In the

presence of edema, the rim appears inseparable on T2WI. It shows rim enhancement on postcontrast T1WI. The degree of hypointensity of the solid caseating tuberculoma on T2W images depends on the complex relationship between the solid caseation, associated fibrosis/gliosis, macrophage infiltration, and perilesional cellular infiltrate. When the solid center of the caseating lesion liquefies, the center appears hyperintense with a hypointense rim on T2WI. The postcontrast T1WI show rim enhancement. MRI features of tuberculomas are known to overlap with those of other intracranial focal lesions, like the healing stage of neurocysticercosis, fungal granulomas, chronic pyogenic brain abscess, and lymphomas. Some gliomas and metastases may also have features similar to those of tuberculomas and should be considered in their differential diagnoses.[20] Sometimes, large tuberculomas mimic neoplastic lesions on MRI as they appear predominantly hyperintense on T2W images, with mixed intensity on T1WI, and may show heterogeneous enhancement on post-contrast studies . Quantitative MT imaging and in vivo proton MRS may help in the differential diagnosis of tuberculomas.

T2 hypointense tuberculomas shows only lipid in vivo spectroscopy, whereas lesions with a heterogeneous appearance show eleavted Choline at 3.22 ppm along with lipid. These lesions show a large amount of cellularity and minimal solid caseation, the cellular regions appearing brighter on MT imaging and showing Choline resonance on Spectroscopy.[21]

METASTATIC DISEASE

80% to 85% of metastases are located in the supratentorial compartment. These lesions may be the direct result of microscopic foci of neoplastic cells transported into the brain via the hematogenous route with subsequent growth in situ, or the metastatic deposit may be primarily to the surrounding calvarium or dural membranes and impinge

on the brain secondarily. The most common type of intracranial space neoplastic lesions are metastases. Most commonly in decreasing incidence, are lung cancer, breast cancer, melanoma, gastrointestinal cancers, renal cell carcinoma, and tumors of unknown primary[22].

Most intracerebral metastases are multiple, regardless of the site of origin; however, there is a high incidence of solitary metastasis, estimated to range from 30% to 50% and especially common in melanoma, lung, and breast carcinoma[23,24]. Surgical intervention is often indicated for solitary metastases whereas radiotherapy or radiosurgery without surgery is generally the therapy for multiple lesions, the detection of intracerebral metastases is critical to patient management. The metastatic foci are often found at gray-white matter junction, i.e a feature of hematogenous spread and also seen in embolic disease. Metastases are notoriously surrounded by massive amounts of edema. The edema accompanying metastases usually does not cross the corpus callosum nor does it involve cortex, features that often help to distinguish these lesions from primary infiltrative brain malignancies.

MR IMAGING

Conventional T2WI rather than FLAIR are best to demonstrate. Intratumoral hemorrhage, which occurs in just less than 20% of metastases [25,26], can be easily detected by MR imaging. Intravenous contrast increases the sensitivity and specificity for the detection of intracerebral metastases. The ring enhancement of a neoplastic lesion characteristically differs from the enhancement of benign conditions, such as abscess, resolving hematoma, and demyelinating disease, by its wall characteristics[27]. Thick, irregular or nodular enhancement are commonly found in malignant neoplasms, but not all neoplasms demonstrate same. As opposed to the regular, thin, even, and smooth enhancing wall denotes benign conditions. It should be stressed that in any patient with a primary extracranial neoplasm and

intracranial enhancement in a nonvascular distribution, metastases should be considered the diagnosis until proven otherwise. The major differential diagnosis of a solitary, thick-walled, ring enhancing lesion in the supratentorial brain of an adult, in the absence of history of prior irradiation, resides in primary glioblastoma versus singular metastasis, a distinction that generally cannot be made on the basis of imaging studies alone.

PILOCYTIC ASTROCYTOMAS

The WHO classifies pilocytic astrocytoma as a grade 1 tumor[28]. There is virtually no evidence of malignant degeneration within this type of tumor. It does not change its aggressiveness with time.

As with any tumor of the CNS, this tumor, if it gains access to the subarachnoid space or to the intraventricular space, can seed and eventually grow, but not aggressively. Pilocytic astrocytomas are the most common glial cell tumors in the pediatric population that arise in the supratentorial space. Pilocytic astrocytomas often predisposes with NF1 syndrome and are commonly seen in the optic chiasm, hypothalamus, and optic nerves. Tumors arising within the diencephalon are most often pilocytic astrocytomas and comprise between 4% and 6% of all pediatric brain tumors[28]. They can also arise within the cerebral hemispheres, with signal and density characteristics that are analogous to those occurring in the cerebellar hemispheres. Thus, they can be both solid and cystic with a mural nodule and can form form ring around the cyst. They may or may not show contrast enhancement. These are tumors that elude proteinaceous fluid from their surface, often producing locules of fluid, giving rise to cysts on the surface of the tumor .The cysts can be more problematic as a mass effect than the solid portion of the tumor .The cysts can dissect into the surrounding brain tissue, displacing structures. The tumor can grow into the cyst, eventually filling it with tumor tissue.

COMPUTED TOMOGRAPHY

The solid portion of the tumor is hypodense relative to cortex and the cystic portion of the tumor is even more hypodense. The solid portion shows contrast enhancement .If it has a disturbed blood–brain barrier. Pilocytic astrocytomas have a significant blood supply.

MAGNETIC RESONANCE IMAGING

Typically the solid portion of these tumors is hypointense on T1 and hyperintense on FLAIR and T2[29,30]. The contrast enhancement is usually brisk. Diffusion imaging shows increased motion of water throughout the tumor with elevated ADC values. Proton spectroscopy shows a mild elevation of choline relative to NAA and relative preservation of creatine.

DEMYELINATING DISORDERS

Several acute demyelinating disorders shows multiple incomplete ring enhancing lesions. They differ in size, shape or pattern and often shows nodular pattern. Some of them demonstrate a ring-enhancing pattern and few have other patterns. None of the neuroimaging patterns just described are specific for multiple sclerosis or other acute demyelinating disorders. The only exception to this is an open ring or incomplete ring lesion. Incomplete or an open ring enhancing lesion helps in differentiating demyelinating lesions from large brain tumors or infective lesions like brain abscess. Atypical ring-enhancing intraparenchymal lesions with mass effect usually undergo brain biopsy to confirm the diagnosis. Otherwise, biopsy of these lesions is not indicated. Conservative treatment corticosteroids often gives favorable outcome in most of the cases.[31,32]

Schwartz KM, Erickson BJ, Lucchinetti C. (2006) studied pattern of T2 hypointensity associated with ring-enhancing brain lesions can help to differentiate pathology The pattern of T2 hypointensity corresponding with ring enhancement was recorded. Gliomas (40%), were the most common pathologies in their study followed by metastases (30%), abscesses (8%) and multiple sclerosis (6%). They concluded that trends in T2 hypointensity may aid in distinguishing among etiologies of ring-enhancing lesions, although there is overlap between the MR appearance of these various pathologies[33].

Vasudev MK, Jayakumar PN, et al. (2007) studied thirty-three patients with intracranial tuberculomas (histologically confirmed in 22) were evaluated using proton density/T2- weighted, T1-weighted (with and without MT), and echo-planar diffusion-weighted imaging sequences. T2 relaxation coefficient (ADC) values. They concluded that Intracranial tuberculomas are characterized by relatively short T2 relaxation times (compared to normal gray matter), decreased MTR, and mostly no restriction of diffusion. A combination of these quantitative parameters could be of help in the noninvasive diagnosis of tuberculomas[34].

Kalita J, Prasad S, Maurya PK, et al. (2012) studied sixty-seven patients with TBM were subjected to clinical, laboratory, magnetic resonance imaging (MRI), and MRA evaluation. They concluded that half the patients with TBM had MRA abnormality involving both anterior and posterior circulations and 61.8% of them had corresponding infarcts[35].

Batra A, Tripathi RP (2004) studied sixteen patients with single or multiple lesions were evaluated on a 1.5T MR system. DWI was performed with three 'b' values of 50, 500, and 1000 s/mm2 and the apparent diffusion coefficient maps were calculated. MR spectroscopy was performed using the point-resolved single-voxel technique with two echotime values of 135ms and 270ms . They concluded that DWI and MR spectroscopy help in determining the nature of cerebral tubercular lesions; however, since the findings

are varied, they do not help in specific characterization[36].

Gupta RK, Husain M, Vatsal DK, et al. (2002) have compared and analyzed the value of in vivo proton MR spectroscopy (PMRS) and T1 weighted magnetization transfer (MT) MR imaging in tissue characterization of brain tuberculomas. We studied 33 cases of proven intracranial tuberculomas with in vivo PMRS and T1 weighted MT MR imaging and concluded that T1 weighted MT MR imaging appears to be more consistent in the tissue characterization of brain tuberculomas[37].

Salgado P, Del Brutto et al. reviewed MR studies of 6 patients with intracranial tuberculoma. While both, CT and MR, were equally sensitive in visualizing the intracranial tuberculoma in every patient, MR was slightly superior in demonstrating the extent of the lesion, especially for brainstem tuberculomas. Nevertheless, the potential role for MR diagnosis of intracranial tuberculoma is limited by the fact that other infectious or neoplasic diseases may present similar findings [38].

Chang KH, Han MH, et al. (1990) reviewed twenty-six patients with intracranial tuberculosis (TB) (10 with acute meningitis, 5 with chronic meningitis, 5 with meningitic sequelae and 6 with localized tuberculoma(s) were examined with MR before and after Gd-DTPA enhancement. MR imaging appears to be superior to CT in evaluation of active intracranial TB only if Gd-DTPA is used, while CT is better than MR in evaluating meningitic sequelae with calcification.[39]

Suh DC, Chang KH, et al. (1992) retrospectively evaluated MR images obtained on a 2.0T superconducting unit in 22 neurocysticercosis patients and observed various MR features including some new findings. A variety of MR findings are presented with special reference to six case reports. The features include: (1) a large simple cyst containing both internal septations and a scolex; (2) suprasellar racemose cysts mimicking other cysts, (3) a fourth ventricular cyst readily depicted by aid of CSF flow-void in the

sagittal plane; (4) degenerating cysts showing "white target" appearance; (5) granulomatous lesions having a "black target" appearance; and (6) a meningitic form showing Gd-DTPA enhancement of basal cisterns and of a subacute infarct[40].

Amaral L, Maschietto M, et al. (2003) retrospectively analysed 172 cases of neurocysticercosis in MR studies was carried out over a period of 13 years. They concluded that MR imaging is a sensitive and specific method in the analysis of different forms of unusual manifestations of neurocysticercosis, which should appear in the differential diagnosis of parenchymal, ventricular, spinal, cisternal, and orbital lesions [41].

Chang KH, Han MH reviewed MRI finding of parasitic disease of the central nervous system (CNS) in 1998, with emphasis on neurocysticercosis which is by far the most common CNS parasitic infection world-wide. They concluded that MRI is superior to CT in the evaluation of most CNS parasitic infections and is nearly diagnostic, particularly in endemic areas. Contrast enhanced studies is essential not only for specific diagnosis of the disease, but also for the assessment of the inflammatory activity[42].

HR Martinez R Rangel- Guerra, et al. reviewed the MR findings in 56 patients with neurocysticercosis (NCC) in 1989, MR finding were correlated with other neuroradiological finding in 40 cases with histopathological studies in 15 surgically treated patients, and with autopsy finding in one case. They concluded that MR is sensitive in diagnosing active NCC and may be useful in evaluating the degenerative changes in parasite that occur as a result of natural degeneration, host response or medical therapy[43].

Haris M, Gupta RK, Singh A, et al. (2008) studied 103 patients with infective brain lesions (group I, n=26) and neoplastic brain lesions (high-grade glioma, group II, n=52; low-grade glioma, group III, n=25) underwent dynamic contrast-enhanced MR imaging.

They concluded that physiological perfusion indices such as k(trans) and v(e) appear to be useful in differentiating infective from neoplastic brain lesions. Adding these indices to the current imaging protocol is likely to improve tissue characterization of these focal brain mass lesions[44].

Savita R Singhal, Smiti Nanda and Suresh K Singhal report the cases of two Indian women, aged 20 and 24 years old respectively, with neurocysticercosis presenting in the second trimester of pregnancy with convulsions. Neurocysticercosis should be considered in pregnant women presenting with seizures which cannot be explained by eclampsia, especially in early pregnancy[45].

D. Pal, A. Bhattacharyya,M. et al. evaluated Conventional MR imaging and in vivo 1H-MR spectroscopy data from 194 patients with pyogenic brain abscesses with ages ranging from 3 to 60 years. They concluded that the presence of AAs on in vivo 1H-MR spectroscopy is a sensitive marker of pyogenic abscess, but its absence does not rule out a pyogenic etiology. The presence of Ac with or without Suc favors an anaerobic bacterial origin of the abscess; however, this may also be seen in some of the abscesses secondary to facultative anaerobes [46].

Mao J, Li J, Chen D, Zhang et al. (2011) studied clinical data of premature infants with central nervous system invasive fungal infection. They concluded MRI-DWI and serial MRIs are helpful in the early diagnosis of candida cerebral abscess and the evaluation of treatment outcome in premature infants[47].

G. Luthra, A. Parihar, K. Nath,S. Jaiswal,K.N. Prasad, et al. (2007) performed a retrospective analysis on 110 patients with surgically proved brain abscesses. Imaging studies included T2, T1, postcontrast T1, DWI and PMRS. They concluded that based on the morphologic, ADC, and metabolite information, it may be possible to differentiate among the pyogenic, tubercular, and fungal brain abscesses [48].

Hakyemez B, Ergin N, et al. (2004) evaluated MRI which was performed in 19 patients (four abscesses, seven glioblastomas, two anaplastic astrocytomas, six metastases). In addition to standard MR sequences, trace DW imaging and apparent diffusion coefficient (ADC) maps were performed. DW MRI can be used to identify a brain abscess and can help to differentiate it from a cystic brain tumor. However, restricted water diffusion is not specific and pathognomonic in the differential diagnosis between abscesses and necrotic tumors[49].

Leuthardt EC, Wippold FJ 2nd, et al. (2002) reviewed the MR images of 5 patients presenting with ring-enhancing lesions that ultimately proved to be brain

abscesses were retrospectively reviewed. Restricted water diffusion, as indicated by hyperintensity on DWI and low ADC, in ring-enhancing lesions assists in differentiating brain abscess from necrotic tumor. This information facilitates stereotactic surgical planning: abscesses should be preferentially centrally aspirated, whereas necrotic brain tumors should have diagnostic tissue biopsied from cavitywalls[50].

Ping H. Lai, Jih T. Ho, Wei L. et al. (2002) reviewed fourteen patients (necrotic or cystic tumor (n= 7); pyogenic abscess (n= 7) who underwent 1.5-T 1H-MRS and diffusion-weighted imaging and had findings of ring-shaped enhancement after contrast agent administration were enrolled in this study. They found 1H- MRS and diffusion-weighted imaging are useful for differentiating brain abscess from brain tumor, but the latter requires less time and is more accurate than is 1H-MRS. 1H-MRS is probably more limited in cases of smaller peripheral lesions, skull base lesions, and treated abscesses[51].

Tsui EY, Chan JH, Cheung YK, et al. (2002) concluded that cerebral abscess may sometimes mimic necrotic tumor and cystic metastases both clinically and radiologically. The imaging findings may be indistinguishable on conventional magnetic resonance imaging, MR Spectroscopy may be used in conjunction with DWI in establishing the correct diagnosis[52].

Fichten A, Toussaint P, Bourgeois P, et al. (2001) analysed the difficulties encountered in the differential diagnosis between brain abscess and brain tumor and their influence on treatment and outcome.

Forty-five adults with brain abscess operated on between 1993 and 1999 were retrospectively reviewed. Preoperative diagnosis was right in 55.6% (25/45), wrong in 22.2% (10/45) and doubtful in 22.2% (10/45). Diffusion-weighted MR imaging was

successfully used in 4 doubtful cases to make the differential diagnosis between abscess and tumor[53].

Kazuhiro Tsuchiya, SayukiInaoka, Yoshiyuki Mizutani, and Junichi Hachiya compared fast FLAIR images with conventional spin-echo images (T1- and T2-weighted) obtained in 20 patients with infectious diseases. They concluded that Fast FLAIR images showed pathologic changes in intracranial infectious diseases better than or as well as conventional T2- and proton density–weighted spin-echo sequences. However, postcontrast T1-weighted spin- echo sequences resulted in better visibility of abscess, meningitis, cysticercosis and epidural empyema than did FLAIR images[54].

Shukla-Dave A, Gupta RK, Roy R, et al. (2001) evaluated fifty-one patients with intracranial cystic lesions (21 abscesses, 20 gliomas, 3 hydatid cysts, 3 arachnoid cysts, 1 case each of glioependymal cyst, xantho-granuloma, infarction and acoustic neuroma) were evaluated with conventional MR imaging and in vivo PMRS. . In vivo PMRS accurately predicted the pathology in 92% of the cases. We conclude that in-vivo PMRS complements imaging in better characterization of cystic intracranial mass lesions[55].

X.Z. Chen, X.M. Yin, L. Ai , et al. (2012) forty- five GBM and 21 solitary metastases were retrospectively identified, with their preoperative routine MR imaging analyzed. According to them combined with qualitative and quantitative analysis of peritumoral T2 prolongation, routine MR imaging can help in the differentiation between brain GBM and solitary MET[56].

Sanjay K. Singh, Norman E. Leeds and Lawrence E. Ginsberg (2002) studied sixty-eight patients referred for suspected leptomeningeal metastases underwent 74 MR imaging studies. Contrast-enhanced fast FLAIR sequences are less sensitive than standard contrast-enhanced T1-weighted MR sequences in detecting intracranial neoplastic

leptomeningeal disease[57].

Marius Hartmann, Olav Jansen, Sabine Heiland, et al. 2001) studied seventeen patients with ring-enhancing cerebral lesions (three abscesses, six glioblastomas, eight metastases) on conventional contrast-enhanced T1-weighted images were examined with echo-planar diffusion-weighted MR imaging. In patients with ring-enhancing cerebral mass lesions, restricted diffusion might be characteristic but is not pathognomonic for abscess, as low ADC values also may be found in brain metastases [58].

Y.M. Tang, S. Ngai , S. Stuckey (2006) reviewed the MR imaging studies of 70 patients with a solitary enhancing lesion, without previous surgery or treatment. They concluded that FLAIR, when interpreted in concert with pre- and postgadolinium T1-weighted images, may be useful in differentiating glioma from metastasis when a solitary enhancing cerebral lesion is present. The presence of nonenhancing adjacent cortical involvement in a solitary enhancing lesion is a frequent and relatively specific sign[59].

C.H. Toh , K.-C. Wei, S.-H. Ng , Y.-L.Wan, et al. (2011) studied DTI was performed in 15 abscesses, 15 necrotic glioblastomas, and 26 cystic metastases. In each lesion, manually segmented into 4 regions of interest (ie, cystic cavity, enhancing rim, and immediate [edema most adjacent to the enhancing rim] and distant zones of edema). DTI is able to differentiate abscess from glioblastoma and metastasis. FA, Cl and Cs outperformed ADC in diagnostic performance comparisons[60].

Kee-Hyun Chang, In Chan Song, Sung Hyun Kim, Moon Hee Han, et al. (1998) evaluated 40 proton MR spectra obtained from cystic contents of various intracranial cystic masses in 39 patients. They concluded that only lactate is commonly observed in a variety of intracranial cystic masses, except for abscess and cysticercosis, in which resonances of acetate, succinate, amino acids and / or unassigned metabolites can be seen in addition to a lactate peak[61].

P.H. Lai, H.H. Weng C.Y, Chen S.S. Hsu, et al. (2008) Fifteen patients with aerobic abscesses were studied on a 1.5T MR scanner using an SV method and an SI method. Proton MR spectra of 15 GBMs with similar conventional MR imaging appearances were used for comparison. Metabolite ratios and maximum Cho/Cho-n, Cho/Cr, and Cho/NAA ratios of the contrast enhancing rim were significantly different and useful in differentiating aerobic abscesses from GBMs by MRSI[62].

W. Hollingworth, L.S. Medina, R.E. Lenkinski, D.K. Shibata, et al. (2004) employed a standardized search strategy to find studies published during 2002–2004.They reviewed studies measuring diagnostic accuracy and diagnostic, therapeutic, or health impact of 1H-MR spectroscopy. The current evidence on the accuracy of 1H-MR spectroscopy in the characterization of brain tumors is promising. However, additional high-quality studies are needed to convince policymakers[63].

Mishra AM, Gupta RK, Jaggi RS, et al. included fifty-two patients [abscesses (n = 29), tumor cysts (n = 20) and benign cysts (n = 3)] who formed the basis for comparative evaluation in this study. They concluded that demonstration of restricted diffusion on DWI with reduced ADC is highly suggestive of brain abscess; however, in the absence of restriction, PMRS is mandatory to distinguish brain abscesses from cystic tumors[64]

Gupta RK, Prakash M, Mishra AM, et al. performed DWI in seventy tuberculomas and tuberculous abscesses in 30 patients were categorized in three groups depending on the intensity in the core of the lesion on T2 weighted images. They concluded that addition of DWI to routine imaging protocol may help in differentiation of tuberculous lesions from degenerating cysticercus granuloma.[65]

METHODOLOGY

Source of Data:

The main source of data for the study are patients from teaching hospital attached to Shri B. M. Patil Medical College, Hospital & Research Center, Vijayapura.

Method of Collection of Data (including sampling procedure if any):

All patients referred to the department of Radio diagnosis with clinically suspected cerebral ring enhancing lesions in a period of 1& 1/2 years from Nov 2018 to April 2020 will be subjected for the study.

Inclusion Criteria:

The study includes

- Contrast MR studies showing cerebral ring enhancing lesions are taken up retrospectively.
- All patients with incidentally diagnosed ring enhancing lesion by CT.
- Cases of all age groups irrespective of sex.

Exclusion Criteria:

The study will exclude

- Patients with claustrophobia.
- Patient having history of metallic foreign body insitu like metallic implants insertion and cardiac pacemakers.

EQUIPMENT AND TECHNIQUE USED

The MRI scan was performed MR PHILIPS ACHIEVA & GE SIGNA 1.5T. They have a Superconducting, Ultra-compact, Active shielded superconducting magnet with a magnetic field strength of 1.5 T. ASSET / SENSE coils was used for acquisition of images.

SEQUENCES:

Axial T1, T2, and FLAIR Spin echo sequences, coronal T2; sagittal T1; Post contrast axial; DWI; T2 GRE, Single and multiple voxel spectroscopy was performed at TE of 35, 144 & 288. The voxel is placed on the lesion so that it covers the maximum area of the lesion in a single and multiple voxel. We used T1 post contrast and PRESS sequences with 5 mm thickness. Spectroscopy was avoided in small lesions which are close to bone.

Special sequences such as CISS 3D, VENBOLD were used as and when required.

Statistical test used:

With 95% confidence level and margin of error of ±15%, a sample size of 32 subjects will allow the study to determine the ___with finite population correction (N=100).
By using the formula:

$$n = \frac{z^2 p(1-p)}{d^2}$$

Where,
Z= z statistic at 5% level of significance
d is margin of error
p is anticipated prevalence rate (50%)

Statistical analysis:

All characteristics were summarized descriptively. For continuous variables, the summary statistics of mean± standard deviation (SD) were used. For categorical data, the number and percentage were used in the data summaries and diagrammatic presentation. If the p-value was < 0.05, then the results were considered to be statistically significant otherwise it was considered as not statistically significant. Data were analyzed using SPSS software v.23 (IBM Statistics, Chicago, USA) and Microsoft office 2007.

RESULTS

Total 50 patients presented with various ring enhancing lesions.

Table 4: Incidence of Various Ring Enhancing Lesions

Lesions	No. of Cases
Tuberculoma	12
Primary Brain Tumour	8
Metastasis	4
Neurocysticercosis	4
Abscess	3
CNS Lymphoma	1

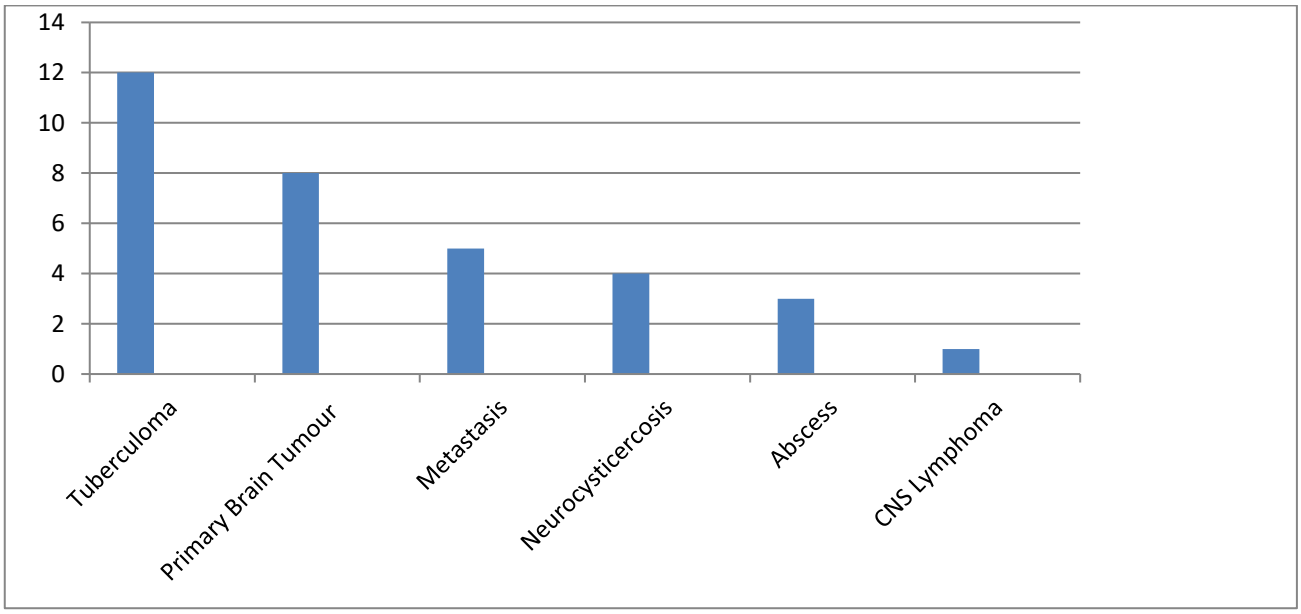

Table 5–Age Wise Distribution of Various Ring Enhancing Lesions

Age (In Years)	No. of Cases
0-10	1
11-20	2
21-30	4
31-40	6
41-50	5
51-60	10
> 61	4

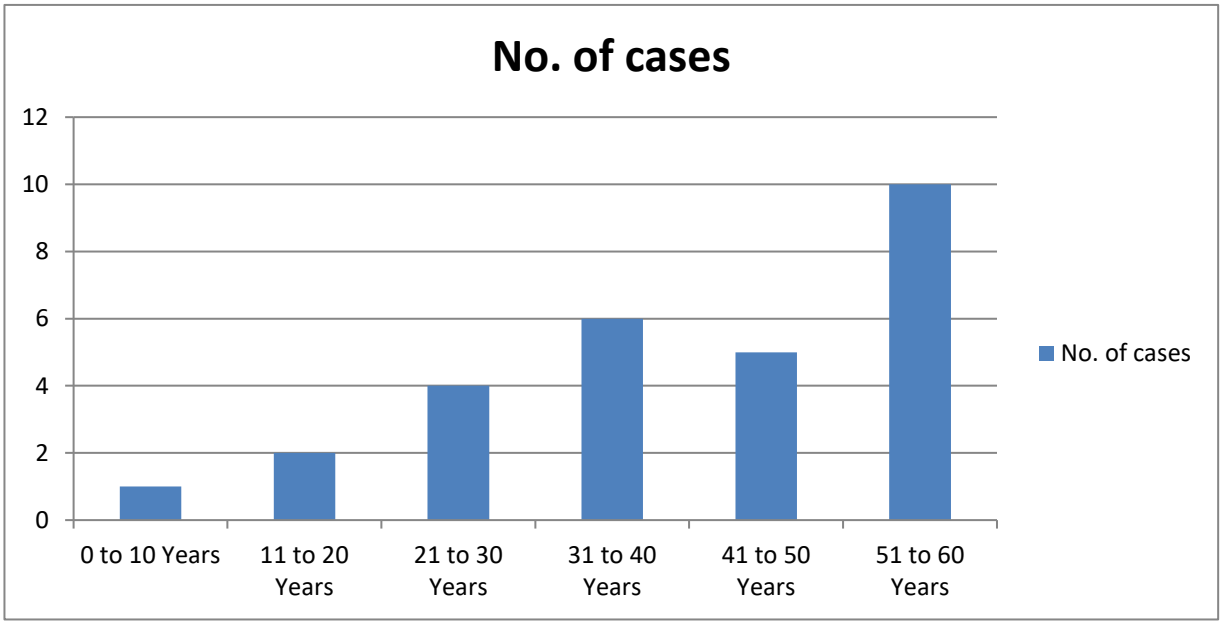

Table 6– Sex wise Distribution of Various Ring Enhancing Lesions

Sex	No. of Cases
Male	20
Female	12

Graph 3: Sex wise Distribution of Various Ring Enhancing Lesions

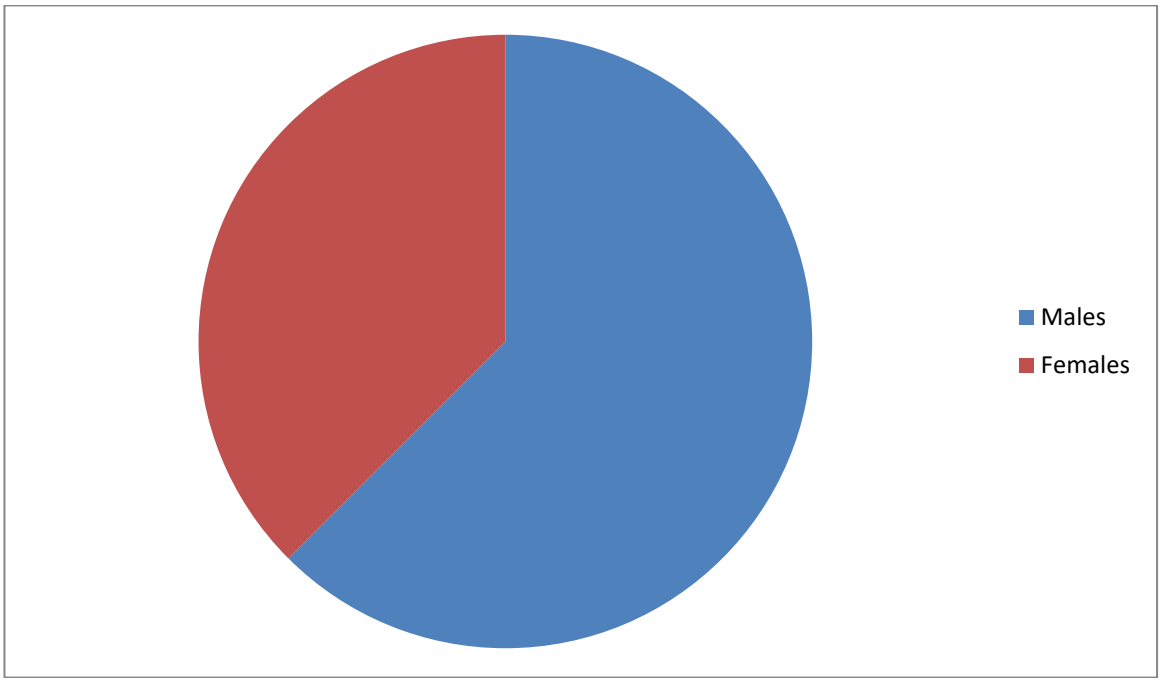

Table 7: Clinical Symptoms Presented by a Patient with Various Ring Enhancing Lesions

Symptom	No. of Cases
Seizures	32
Headache	25
Vomiting	19
Weakness	2
Fever	13
Ataxia	6

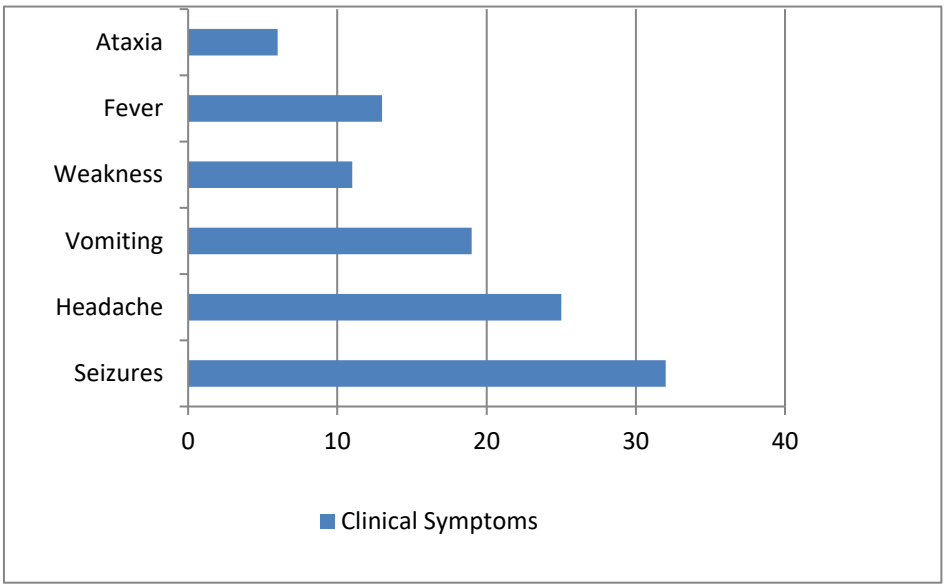

Table 8: Location of Side of Pathology in Brain in Various Ring Enhancing Lesion

Side of Pathology	Number of Cases
Right	8
Left	12
Bilateral	8
Midline	4

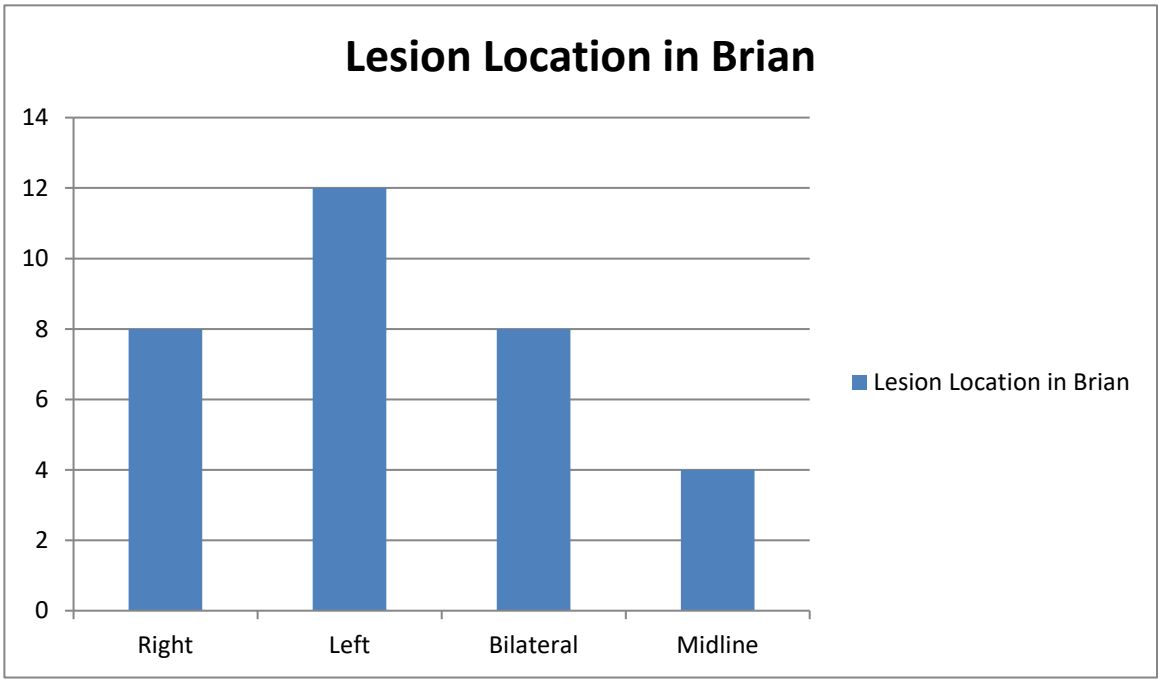

Table 9 –Male Female Incidence of Ring Enhancing Lesions

Pathology	Males	Females	Total
Tuberculoma	9	3	12
NCC	1	3	4
Abscess	3	0	3
Metastasis	1	3	4
Primary Brain Tumour	5	3	8
Lymphoma	1	0	1

Graph6: Male Female Incidence of Ring Enhancing Lesions

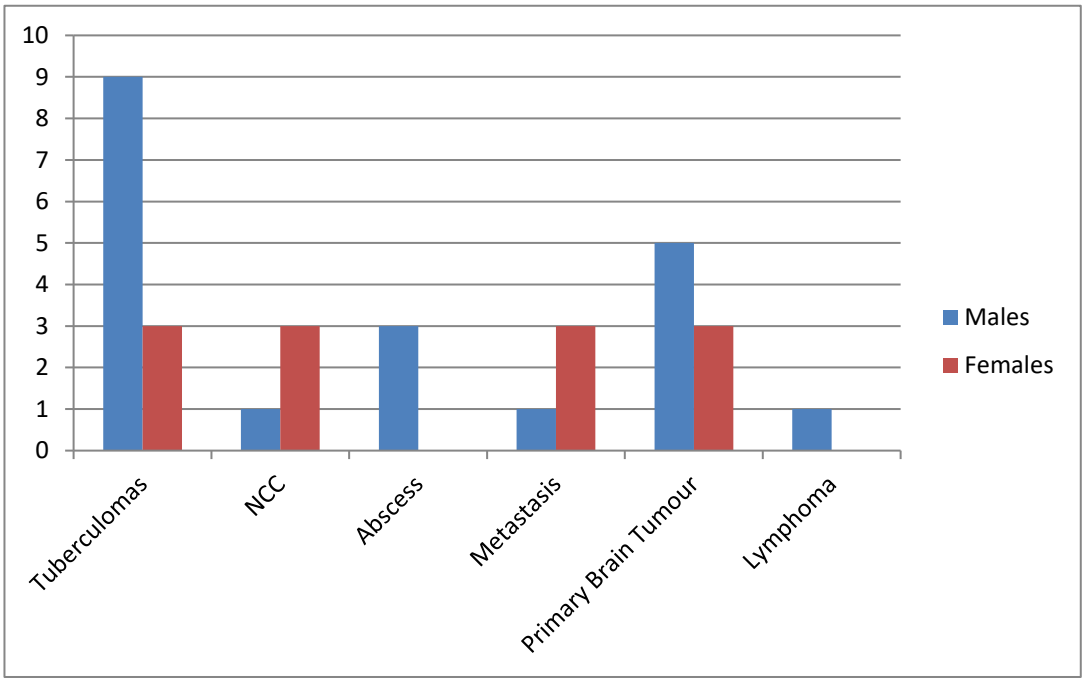

Table 10 – Number of Ring Enhancing Lesions in a Patient

Number of Lesions	Number of Cases
1	12
2-4	06
>4	14

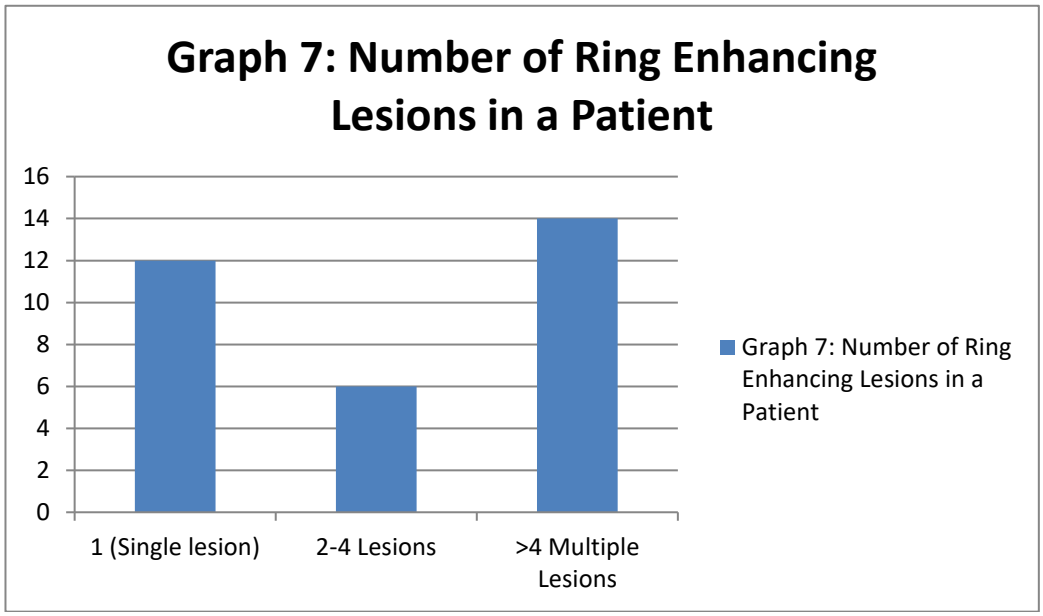

Table 11: Size of Lesion of Various Ring Enhancing Lesions

Size of Lesion (In Cms)	Number of Lesions
< 2	11
2-4	11
>4	10

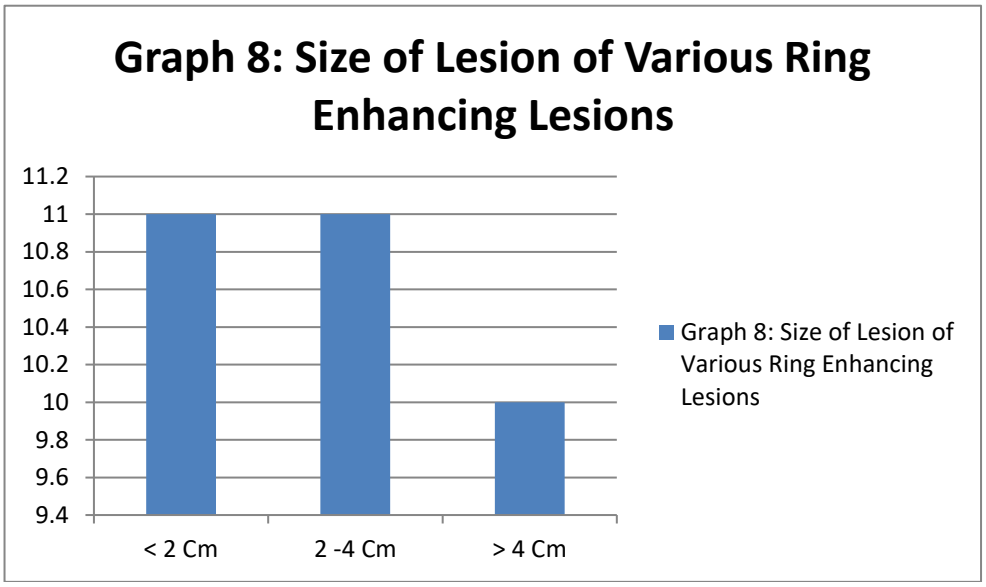

NOTE: In case of multiple ring enhancing lesions, size of the maximum no. of lesions were considered.

Table 12: DWI in Ring Enhancing Lesions

Diffusion	Number of Cases
Showing Restriction (Complete / Partial)	20
Showing No Restriction	12

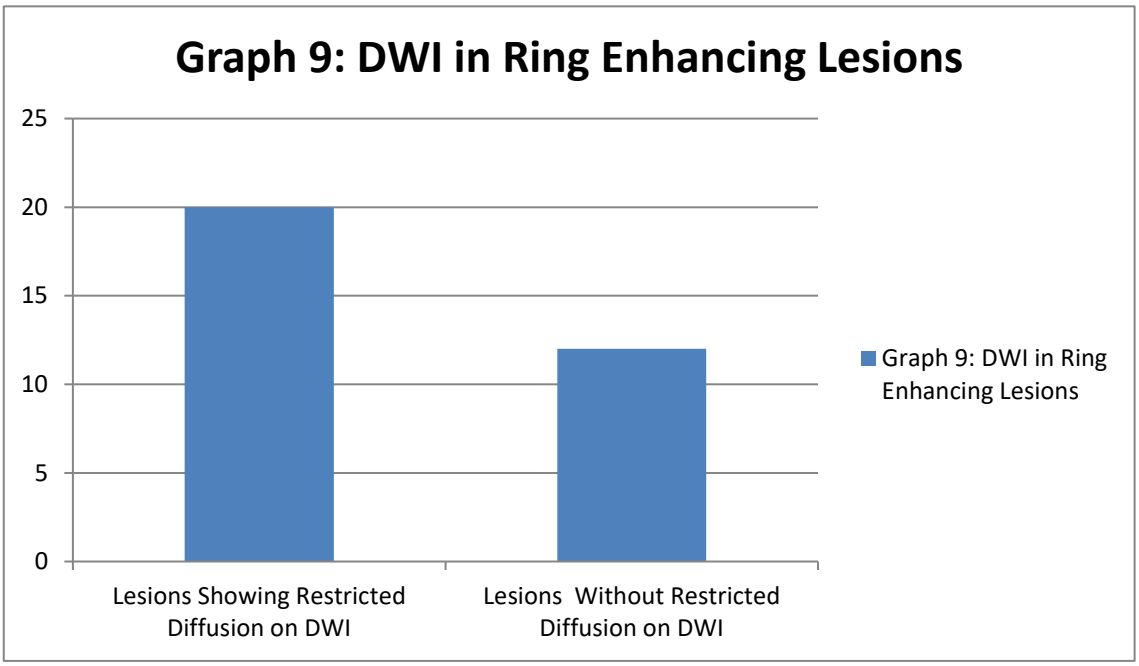

Table 13: List of Various Metabolite Peaks Noted in Various Enhancing Lesions

Metabolite Peak	Number of Cases
Choline	15
Lipid	23
Lactate	24
Reduced NAA	15
Amino Acids	7

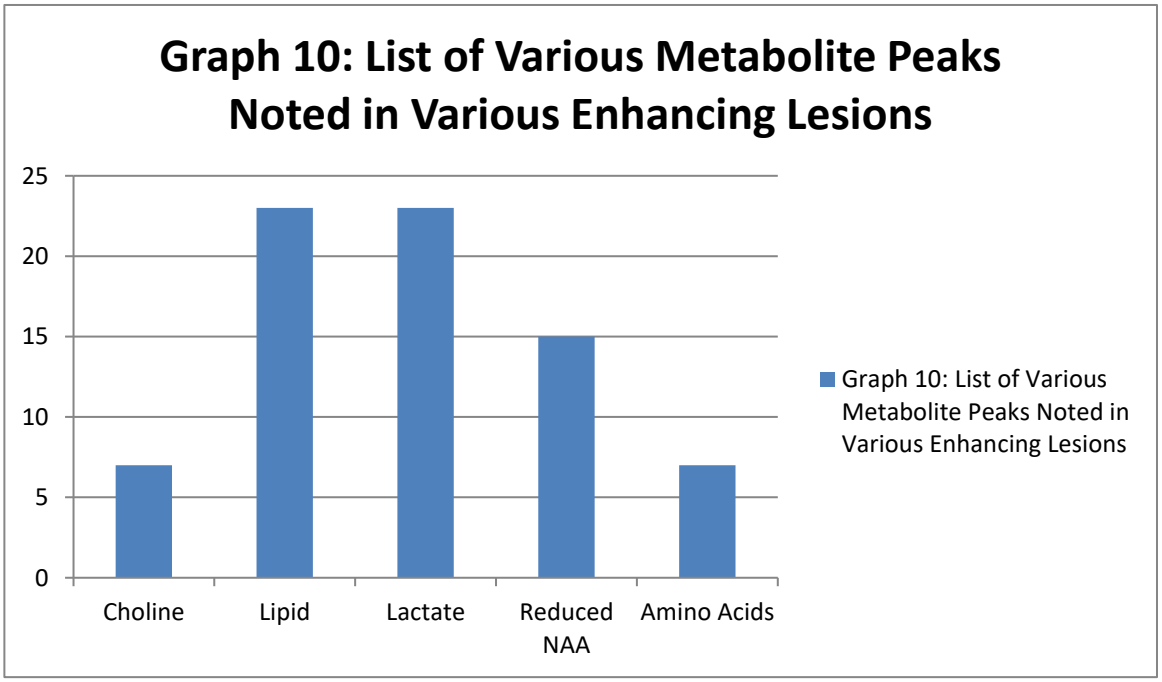

PHOTOGRAPHS

IMAGE 3: PHILIPS ACHIEVA – 1.5 T MRI UNIT

IMAGE 4: GE SIGNA – 1.5 T MRI UNIT

IMAGE 5:

SAGAR - Tuberculoma

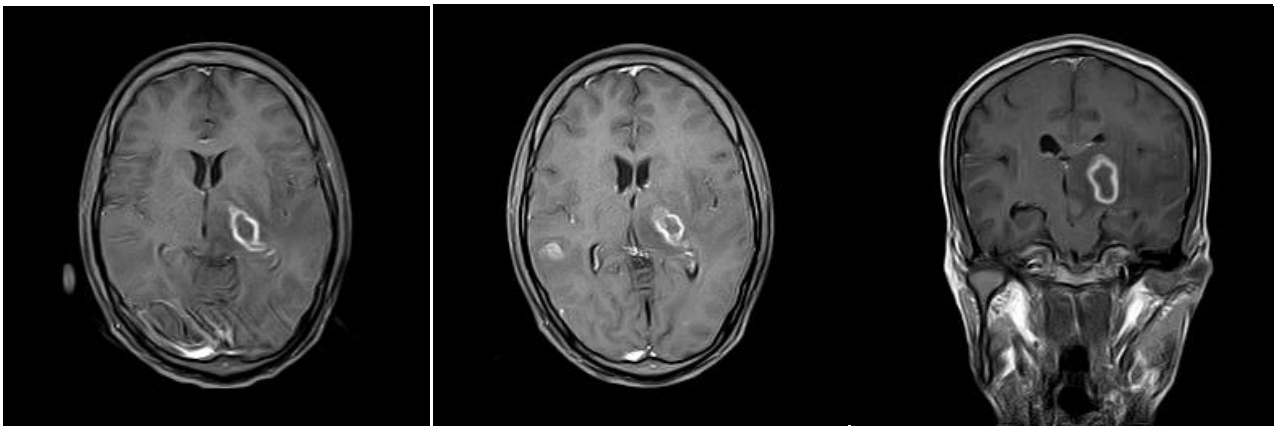

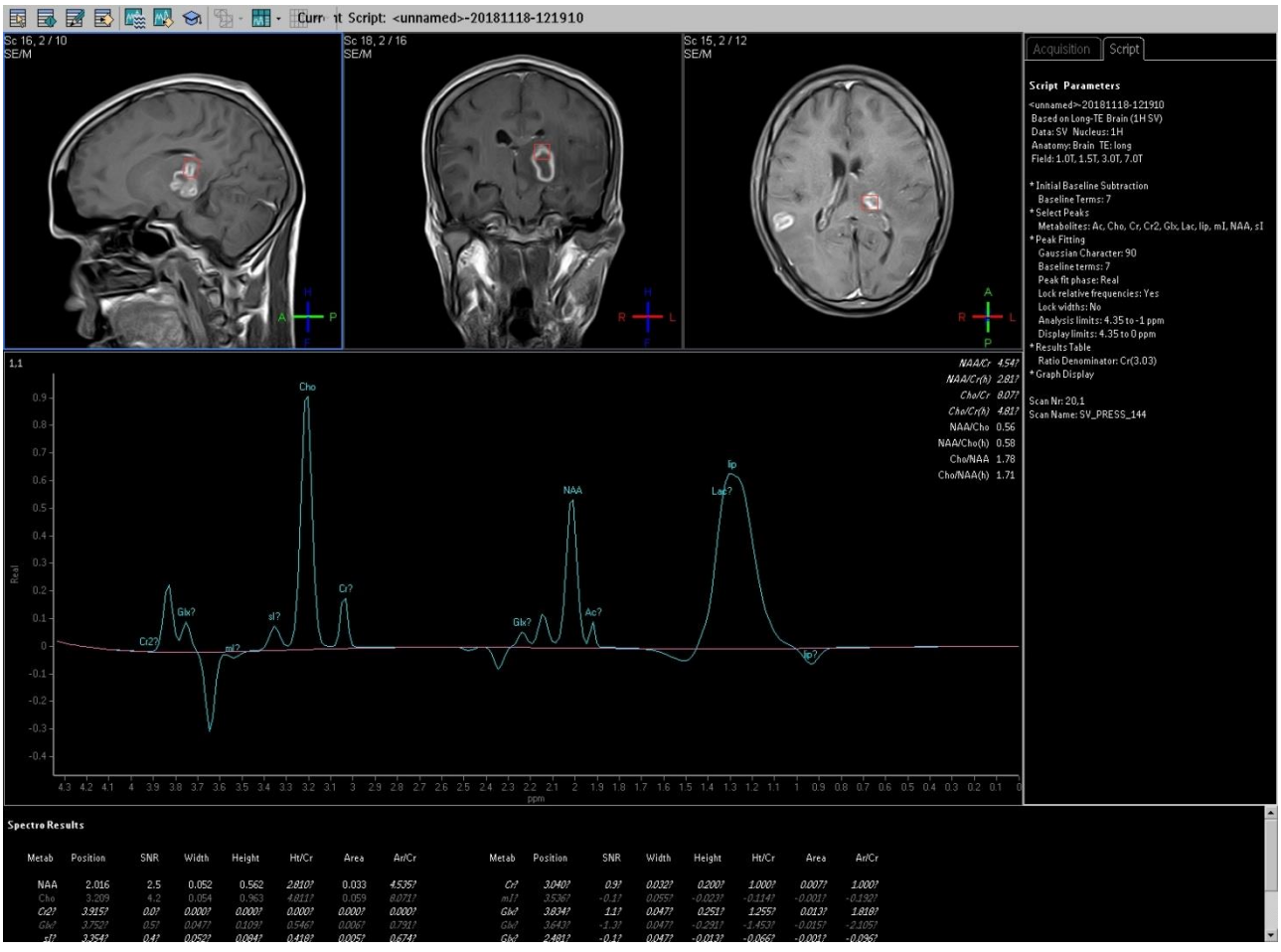

Few ring enhancing lesions in the left thalamo-gangilonic regions and right tempero-parietal lobes showing elevated lipid , lactate and choline levels on spectroscopy- suggestive of tuberculomas.

IMAGE6:

MAHESH -Tuberculoma

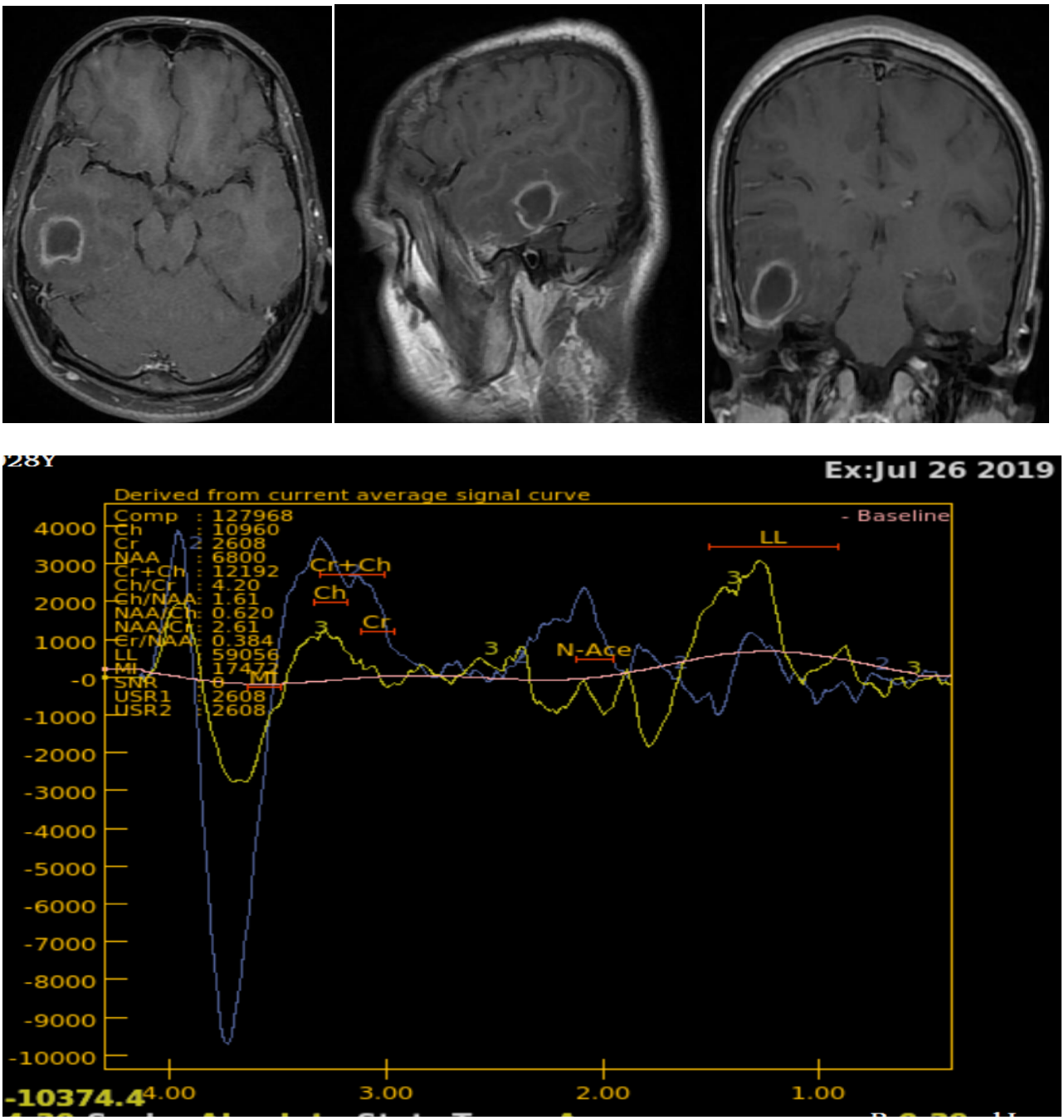

A thick walled irregular ring enhancing lesion with perilesional edema is noted in right temporal lobe. MR Spectroscopy shows lipid ,lactate peak - suggestive oftuberculoma.

IMAGE 7

SIDDARTH – Abscess

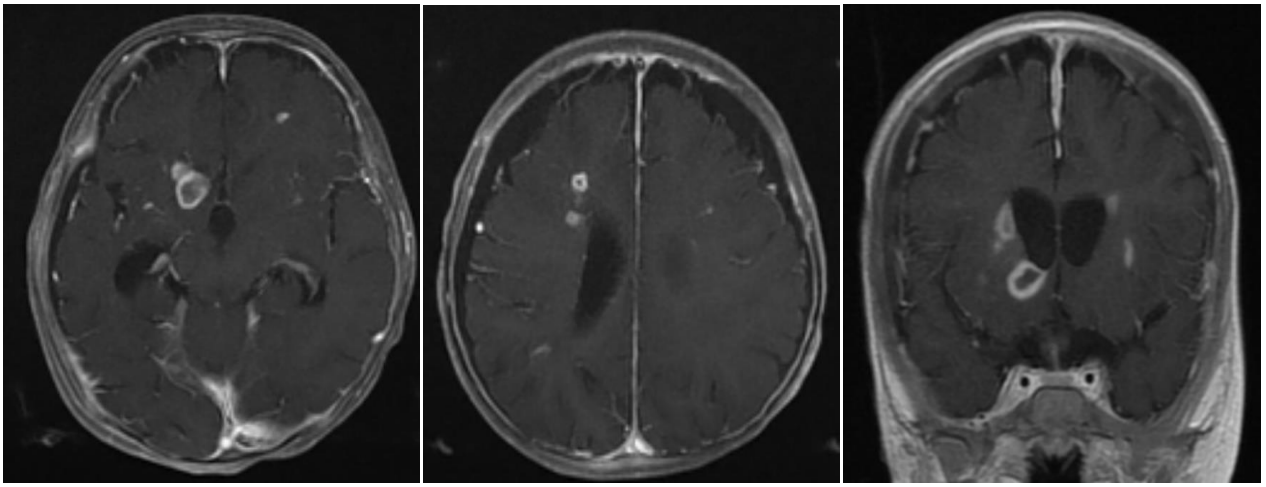

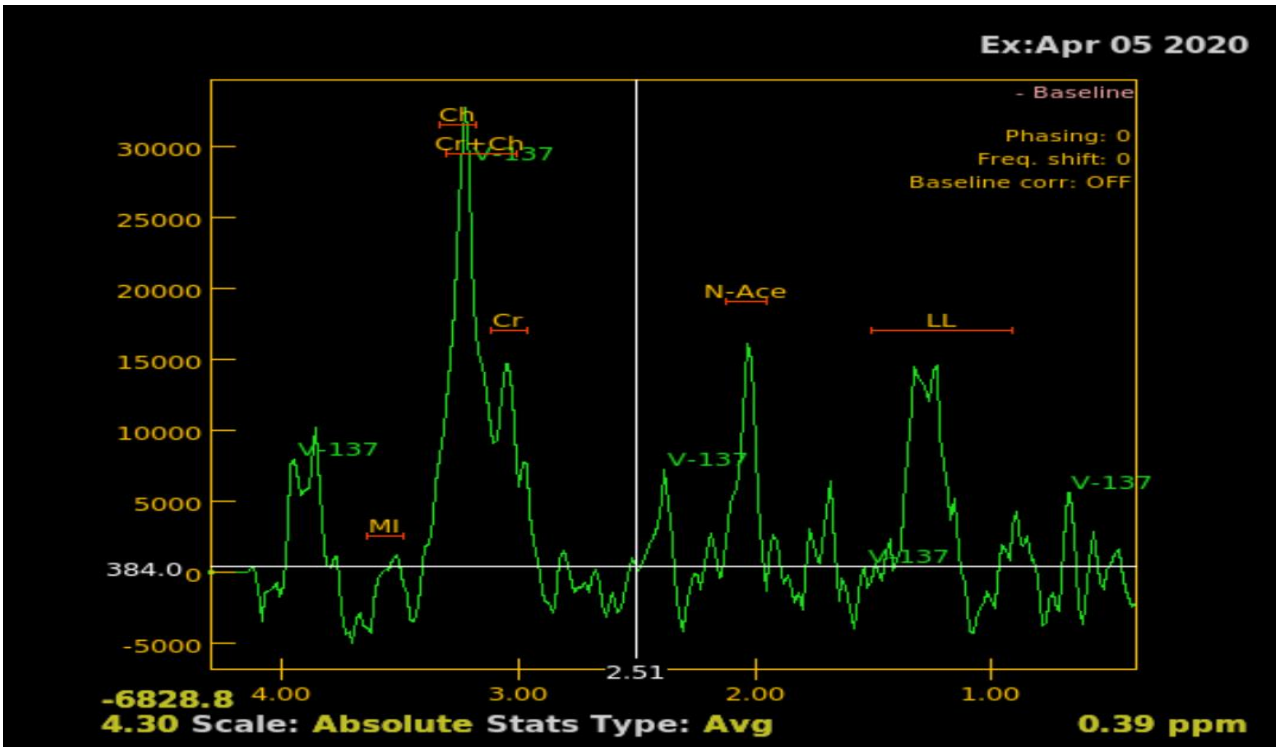

Multiple ring enhancing lesionsshowing elevated lipid lactate with inversion of Choline creatine ratio, increased glutamine and succinate (amino acid)-suggestive of Cerebral Abscess.

IMAGE 8

SAROJINI - NCC.

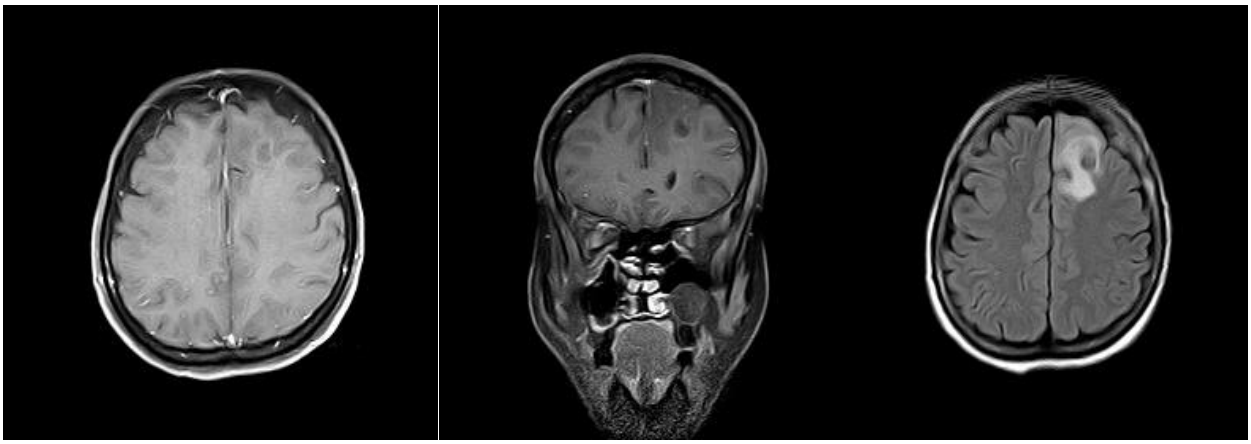

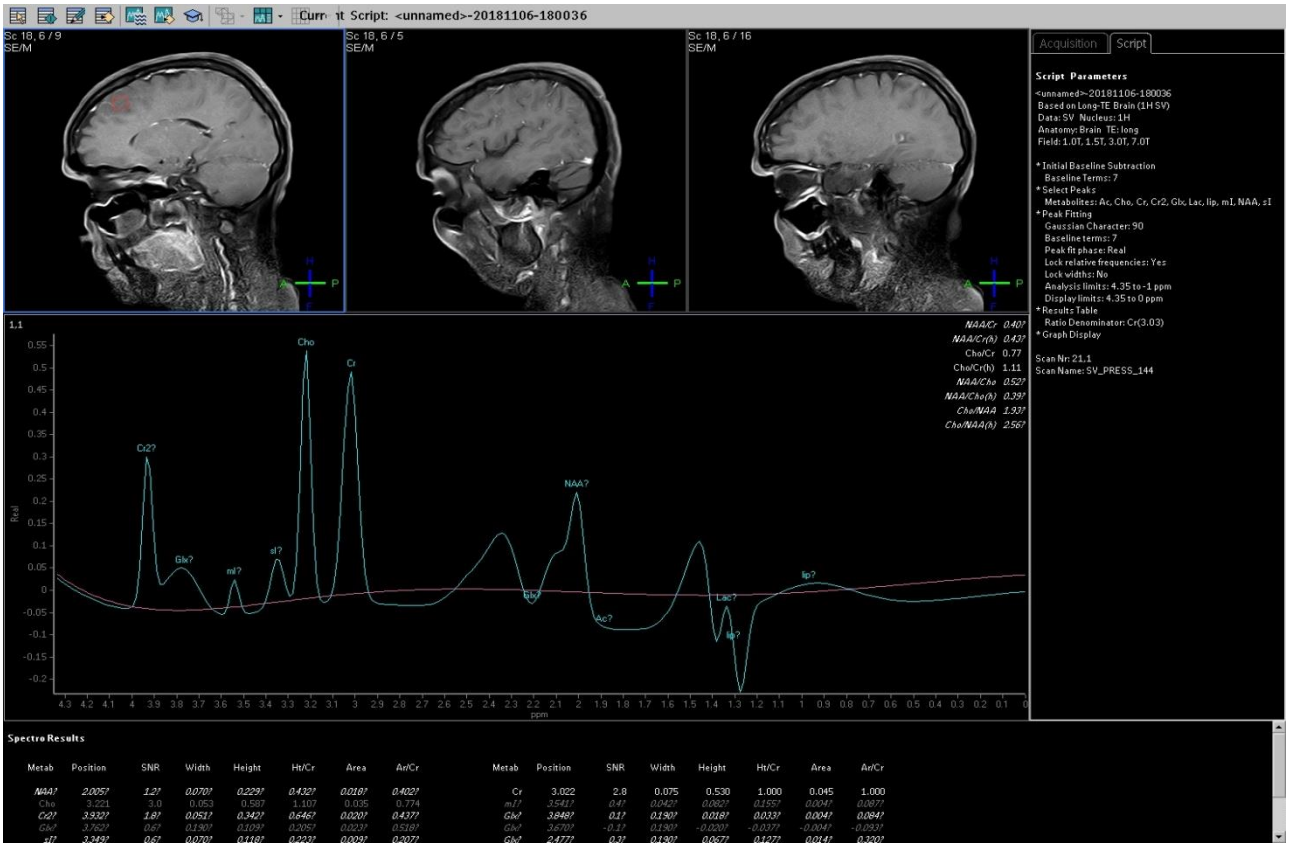

An ill defined hypointense lesion with ring enhancement on post contrast study.

MRS shows inversion of lipid lactate peak, succinate peak & reduced NAA - suggestive ofNCC.

IMAGE 9

Shantabai – Metastases

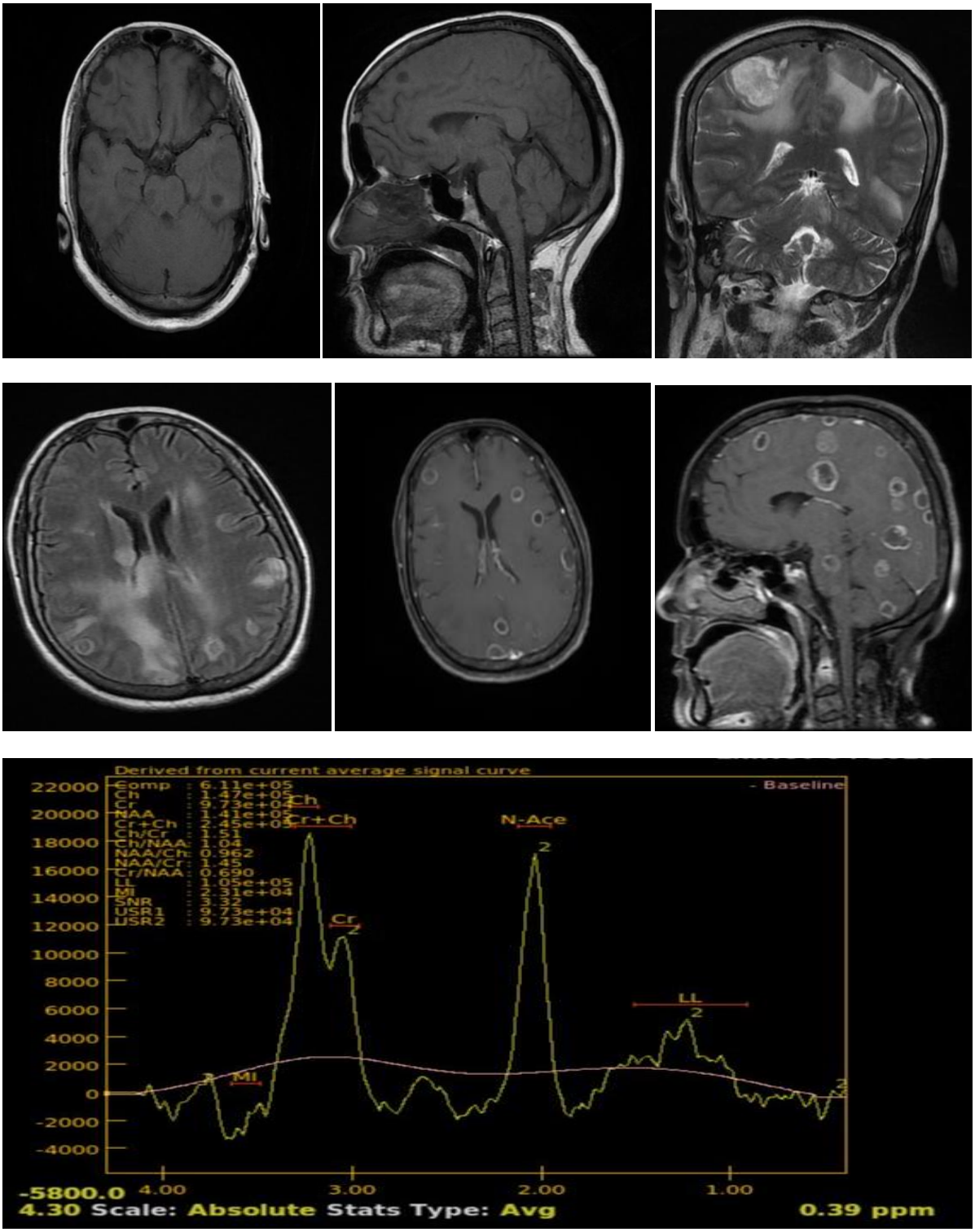

Multiple thick walled ring enhancing T1 hypointense / T2 hyperintense lesionswith significant peri-lesional edema (FLAIR hyperintensities) & spectroscopy showing high choline , NAA and lipid lactate levels - suggestive of metastasis.

IMAGE 10

SHRISHAIL- High Grade Glioma (Primary brain tumor)

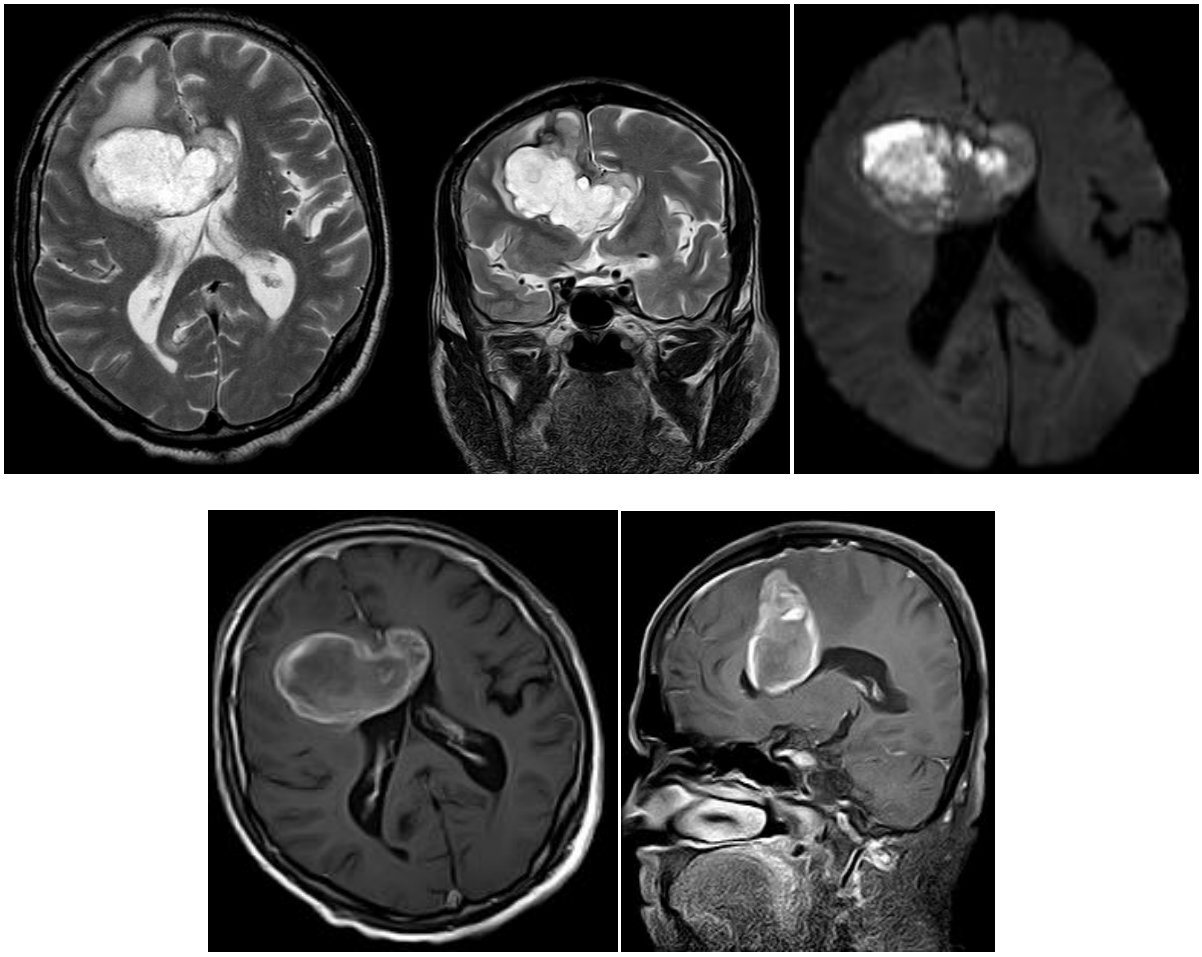

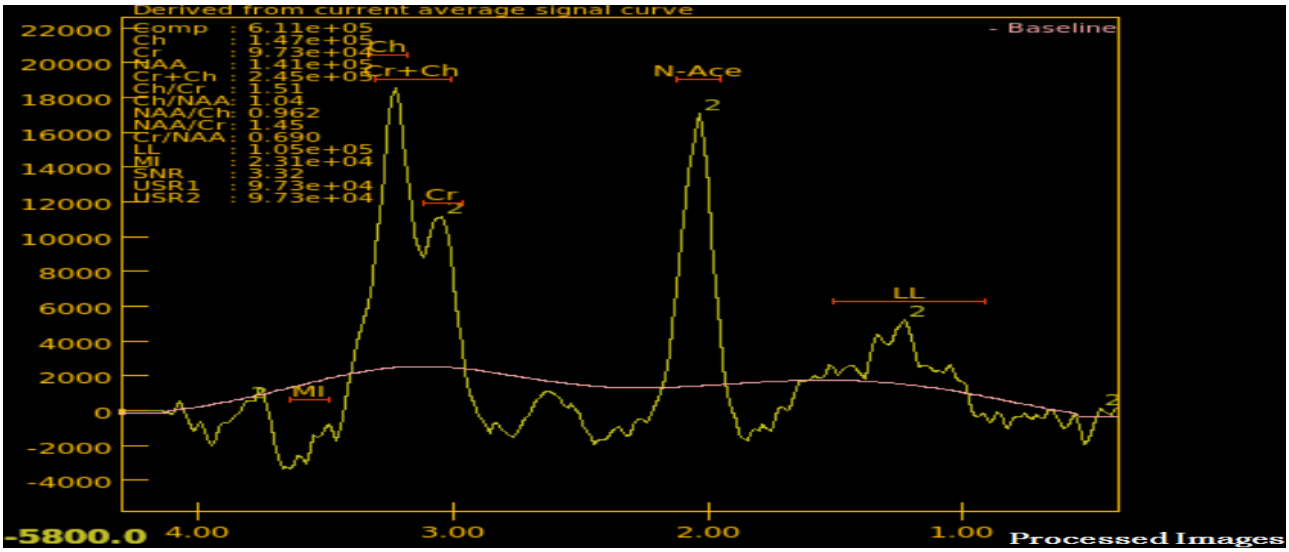

A large T2/FLAIR hyperintense lesion in right frontal lobe crossing midline showing thick irregular ring enhancement and on post contrast study shows elevated choline, NAA and lipid lactate peak - suggestive of high grade glioma.

IMAGE 11

KASHIMALI- CNS Lymphoma

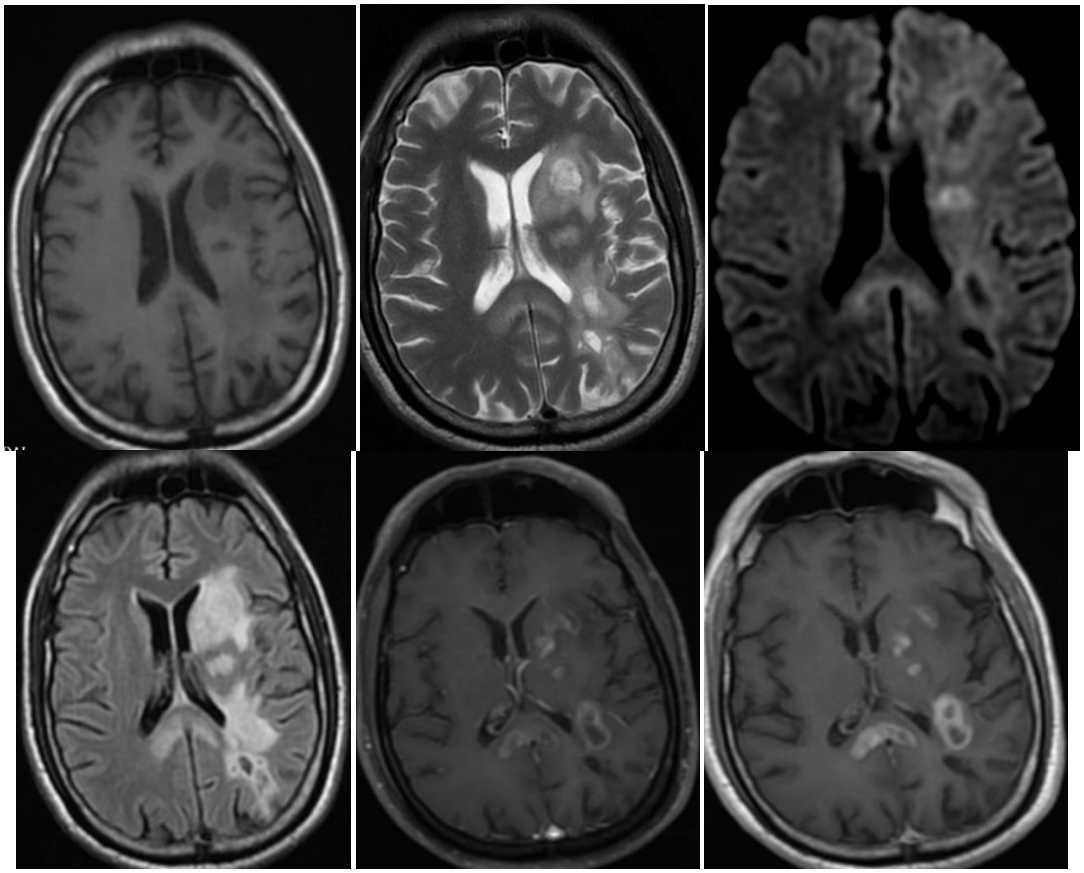

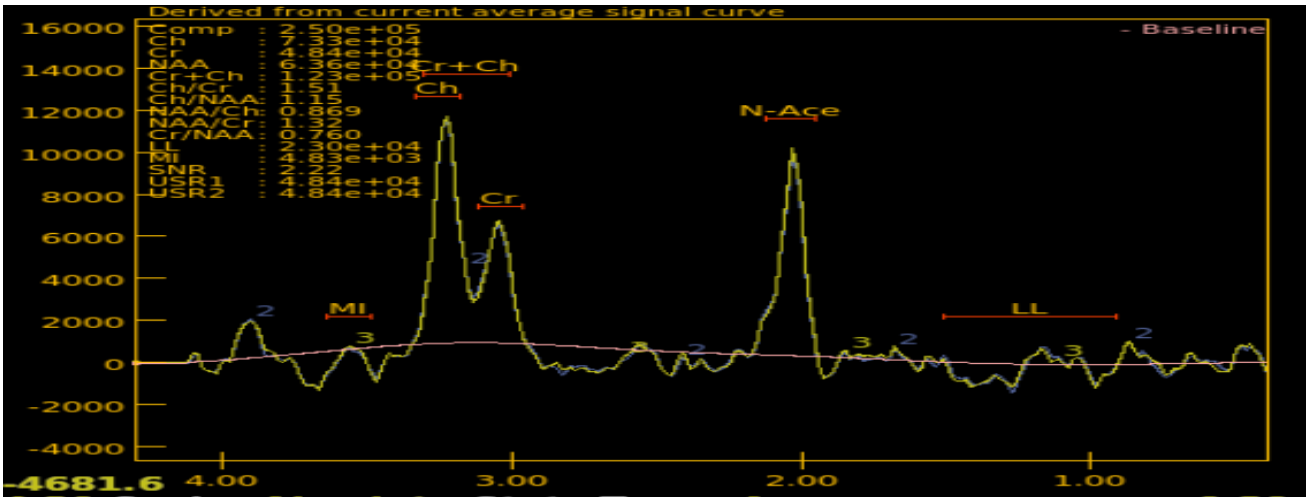

Multiple ring enhancing lesions appearing T1 hypointense/ T2 hyperintense lesions showing peripheral diffusion restriction and significant peri-lesional edema (FLAIR hyperintensities) in the periventricular area of left frontal, capsule-ganglionic, peri-trigonal regions and splenium of corpus callosum. On MRS shows choline peak, increase Choline/creatine ratio, NAA and mild increase in lipid lactate levels - suggestive of CNS Lymphoma.

DISCUSSION

MRI is a multiplanar, noninvasive and highly accurate method to demonstrate the intracranial lesion and with help of contrast and spectroscopy it adds additional information. It provides an accurate assessment of various ring enhancing lesions in the brain and aid in diagnosis with immediate introduction to the treatment.

This was a prospective study done in the Department of Radiodiagnosis and Imaging, Shri B. M. Patil Medical College, Hospital & Research Center, Vijayapura we evaluated 32 patients and aimed at studying the MR appearances with spectroscopic changes of various ring enhancing lesions in the brain.

AGE DISTRIBUTION

A total of thirty two patients were evaluated prospectively, with an age group ranged from 10 months to 76 years. The incidence of ring enhancing lesions were found highest in 51-60 years age group accounting for 37.5% of cases and least in 0-10 years age group constituting 3.2%.

SEX DISTRIBUTION

A total of thirty two patients were evaluated with incidence higher in males than females. 20 were males (62.5%) and 12 (37.5%) were females.

CLINICAL FEATURES

Seizures are the most common presenting complaint in 84 % of cases. Headache (22%), fever (18%), vomiting (6%), ataxia (8%) and motor weakness (6%) were the other presenting complaints.

PATHOLOGIES

Out of the 32 patients who were evaluated, tuberculomas (37.5%) was the most common pathology followed by primary brain tumour (25 %), NCC (12.5%), metastasis (12.5%), Abscesses (9%), and Lymphoma (3%).

In a study conducted by Schwartz et al[33] 40% cases were gliomas. The higher incidence of tuberculomas is probably due to the higher prevalence of tuberculosis in India.

SIDE OF LESION

Among the thirty two patients with RELs noted 8 (25%) were noted on the right side, 12 (37.5%) were noted on the left side, 8 (25%) were seen bilaterally and 4 (12.5%) in the midline.

NUMBER OF LESIONS

Thirty two patients were evaluated - 12 (37%) of them presented with a single lesion. 2-4 lesions were noted in 6 (19%) of cases and > 4 RELs were seen in 14 (44%) of cases.

SIZE OF THE LESION

Thirty two patients were evaluated - majority 11 (34%) of them showed RELs < 2cm, 11 (34%) of them showed lesions of sizes between 2-4 cm and only in 10 (32%) lesions size is greater than 4 cm.

In case of multiple lesions size of the maximum number of lesions which were falling in one category were considered.

DIFFUSION RESTRICTION

Thirty two patients were evaluated - 20 (63%) of patients show diffusion restricting lesions (partial/complete) and 12 (37%) of cases shows no diffusion restriction.

MR SPECTROSCOPY

Thirty two patients evaluated with MR spectroscopy. Choline peak was observed in 15 cases, Lipid in 23 cases, Lactate in 24 cases, reduced NAA peak in 15 cases and amino acids in 7 cases.

TUBERCULOMA

Out of thirty two patients evaluated tuberculomas were seen in 12 (38%) of cases. Among the 12 cases (males = 9: females = 3). Single lesions were noted in 3 cases (25%) and multiple in 9 cases (75 %). They are seen as conglomerate lesions which are hypointense on both T1 and T2. OnT1 weighted images they show a iso to hyperintense ring which was seen in 9 cases in our study. They may show partial or complete restriction seen in 9 cases – 75%.

The lesions may show a nodular or irregular ring like enhancement. All our cases

presented with presented with ring like enhancement. Nodular enhancement is also seen in 2 cases in addition to the ring enhancing lesions. MRS showed a Lipid peak in 12 (100%) cases and it plays an important role in identification of tuberculomas from other infective granulomas. The stage of the tuberculoma whether it is caseous or non caseous can also be identified on MRI with the help of T2 weighted images. Post contrast images are very helpful in identifying the size of the tuberculomas due to its excellent spatial resolution and differentiates the granuloma from its surrounding edema.

Tae Kyoung Kim , Kee Hyun Chang, Chong Jai Kim, Jin Mo Goo, MyeongCherl Kook, and Moon Hee Han (1995) showed that on T1-weighted images, the granulomas showed a slightly hyperintense rim. On T2-weighted images, the entire portion of the granuloma showed slightly heterogeneous isointensity or hypointensity with small markedly hypointense foci. On postcontrast T1-weighted images, there were single or multiple conglomerate ring enhancements within a tuberculoma in all sixpatients.[66]

Jayasundar R, Singh VP, Raghunathan P, Jain K, Banerji AK (1999). concluded that presence of lipid can be used for differentiating tuberculomas from both non-specific IG and NCC.[67]

Follow up scan (CT/MRI) was performed in 16 patients which showed resolution of the lesion as well as peri-lesional edema.

NEUROCYSTICERCOSIS

Out of thirty two patients evaluated neurocysticercosis was seen in 4 (males=1; females=3) cases. 2 patients presented with single lesions whereas

2 patients presented with multiple lesions. All the cases were showing intraparenchymal forms of NCC with no spinal cysticercosis or subarachnoid cysticercosis. Scolex was identified in 1 case using CISS 3D sequence. MRS shows Choline peak and elevated NAA peak. Gradient echo imaging played a significant role in identifying calcified lesions which were seen in 1 case (25 %). All the lesions were hypo to isointense on T1 weighted images and 3 were hyperintense on T2. Out of these 12 lesions 9 lesions showed inversion on FLAIR suggesting that the contents are similar to that of CSF. Intense ring enhancement with surrounding perilesional edema was seen in all cases suggestive of active lesions.

We did not find a single case of intraventricular cysticercosis probably because of the small sample of study. Martinez et al reported intraventricular neurocysticercosis in 22 % of cases.[43]

Parenchymal cysticercosis is better identified on MRI than CT in our study as compared to the study done by Suss Ra et al.[68]

Features of parenchymal forms of NCC in our study are similar to the study done by do Amaral LL et al.[41]

Cho / Cr ratio was less than 1.1 in all NCC and more than 1.2 in all tuberculoma which is similar to the study performed by Kumar et al and Jayasunder et al[69,70]

ABSCESS

Out of the 32 patients, abscess were found in 3 cases – 100 % (males =3; females =0). Single abscess was found in 1 cases (33%) whereas the other 2 cases had multiple abscesses. All the cases showed sizes >2 cm and one case was >3 cm. All were hypointense on T1 weighted images with a hyperintense rim noted in all 3 patients and were hyperintense on T2 weighted images with a surrounding hypointense rim (all 3 cases). They showed complete diffusion restriction and MRS showed Lactate peak in all 3 cases suggesting anaerobic glycolysis with amino acids like glutamine seen in all 3 cases.

Halmes et al described the appearance of abscesses on MR. We correlated our findings with those described and distinguished the peripheral edema, central necrosis and the characteristic pattern of peripheral enhancement of the abscess capsule.[71]

Our findings were similar to the study conducted by Tsui EY et al, Shukla-Dave A et al (55) and Leuthardt EC et al[50].

METASTASIS

Out of the 32 patients, 4 cases were metastasis (males = 1 ; females=3). Multiple lesions were identified in all the 4 cases. All the cases showed high Cho / Cr and Cho/NAA levels . All 4 cases were heterogenously hyperintense on T2 with peripheral rim of FLAIR hyperintensities. Primary was identified in 3 cases one from breast and other two from lung . Thick, irregular type of ring enhancement was noted after contrast administration. Our findings were similar to the study conducted by Vieth RG et al[27]

LIMITATIONS

- MR perfusion and MTR which were not included in the study are also useful in differentiation of neoplastic and non neoplastic lesions.
- Most of our cases 22 (69%) were < 4 cm, so single voxel spectroscopy was sufficient. But in larger lesions multivoxel spectroscopy helps in differentiating the characteristics of the internal contents as well as the wall.

CONCLUSION

- MRI is the most sensitive modality in the characterization of intracranial ring enhancing lesions –RELs
- Irregular type of ring enhancement is the most common feature noted in most of the lesions.
- Most common lesion seen is Tuberculoma (38%) followed by primary brain tumour (high grade glioma) (25%), neurocysticercosis (12.5%), metastasis (12.5%), abscess (9%) and CNS lymphoma (3%).
- 51-60 years is the most common age group involved (32% of cases) and seizures is the most common presenting complaint (100%).
- Single lesion was noted in 38 % of patients whereas the rest 62% presented with multiple cases.
- Pattern of signal intensity on T2 and FLAIR, DWI and MRS help to differentiate between benign and malignant lesions.
- Hypointensity on T2 with partial or complete restriction on DWI images and lipid peak on MRS is more in favour of Tuberculoma.
- Hyperintensity on T2 with no diffusion restriction, presence of scolex on CISS 3D suggests NCC.
- Abscesses show a hypointense rim on T2 with complete diffusion restriction. MRS may show elevated lactate and amino acids.
- Metastasis are well defined hyperintense lesions on T2 which show high choline peak on MRS.
- MRI being non invasive and non- radiating is an ideal imaging modality.

- CISS 3D and MRS are to be routinely used in evaluation of ring enhancing lesions.
- Multiplanar capability of MRI was helpful in identifying precise anatomical location and the exact extent of lesions.
- MRI plays a critical role in patient management by suggesting the correct diagnosis based on characteristic imaging findings.
- MRS helps in characterization of various ring enhancing lesions. However no lesion can be diagnosed based on the findings of MRS as the sole criteria.

SUMMARY

Thirty two patients with ring enhancing lesions on MRI (10 cases were referred to MRI after prior CT showed ring enhancing lesions) were evaluated in this study conducted over a period of 1 & ½ years from Nov 2018 to Apr 2020 of various age groups ranging from 10 months to 76 years. MRS was performed in all 32 cases. Various parameters of ring enhancing lesions were evaluated. Spectrum of findings on MRI and MRS were assessed.

- Out of 32 cases, 12 are tuberculomas, 8 are primary brain tumours, 4 each are NCC & metastasis, 3 are abscess and 1 case of CNS lympohoma.
- Males were predominantly affected (20 cases - 63% of cases) than females (12 cases - 37 %).
- T2 signal intensity, DWI and MRS plays a very important role in characterization of ring enhancing lesions.
- Seizures are the most common clinical presentation noted in all cases.
- Follow up CT / MRI in 12 patients shows resolution of the lesion and its associated peri-lesional edema.

BIBILOGRAPHY

1. Omuro AM, Leite CC, Mokhtari K, Delattre JY. Pitfalls in the diagnosis of brain tumours. Lancet Neurol2006;5:937-48.
2. Cunliffe CH, Fischer I, Monoky D, Law M, Revercomb C, Elrich S, et al. Intracranial lesions mimicking neoplasms. Arch Pathol Lab Med 2009;133:101-23.
3. Smirniotopoulos JG, Murphy FM, Rushing EJ, Rees JH, Schroeder JW. Patterns of contrast enhancement in the brain and meninges. Radiographics 2007;27:525-5
4. Bulakbasi N. Clinical applications of proton MR spectroscopy in the diagnosis of brain tumours. Spectroscopy 2004;18(2):143-153.
5. Zee CS, Segall HD, Boswell W, et al. MR imaging ofneurocysticercosis. J Comput Assist Tomogr 1988:12:927-934
6. Sortelo J, Escobedo F, Penagos P. Albendazole vs. praziquantel for therapy for neurocysticercosis: a controlled trial. Arch Neural 1988;45:532-534
7. Martinez HR. Rangel-Guerra R, Elizondo G, et al. MR imaging in neurocysticercosis: a study of 56 cases. AJNR1989:10:1011-1019
8. Teitelbaum GP, Otto Ri, Watanabe AT, et al. MR imaging of neurocysticercosis. AiR 1989:153:857-866
9. PanditS,Lin A, Gahbauer H, LibertinCR,Erdogan B. MR spectroscopy in neurocysticercosis. J Comput Assist Tomogr 2001; 25:950-952.
10. Sze G, Zimmerman RD. The magnetic resonance imaging of infections and inflammatory diseases. RadiolClin North Am1988;26:839–859

11. Haimes AB, Zimmerman RD, Morgello S, et al. MR imaging of brain abscesses. AJR Am J Roentgenol1989;152:1073–1085

12. Desprechins B, Stadnik T, Koerts G, et al. Use of diffusion-weighted MR imaging in differential diagnosis between intracranial necrotic tumors and cerebral abscesses. AJNR Am J Neuroradiol 1999;20:12521257.

13. Kim YJ, Chang KH, Song IC, et al. Brain abscess and necrotic or cystic brain tumor: discrimination with signal intensity on diffusion-weighted MR imaging. AJR Am J Roentgenol1998;171:1487–1490.

14. Dev R, Gupta RK, Poptani H, et al. Role of in vivo proton magnetic resonance spectroscopy in the diagnosis and management of brain abscesses. Neurosurgery1998;42:37–42

15. Kim SH, Chang KH, Song IC, et al. Brain abscess and brain tumor: discrimination with in vivo H-1 MR spectroscopy. Radiology 1997;204:239–245.

16. Poptani H, Gupta RK, Jain VK, et al. Cystic intracranial mass lesions: possible role of in vivo MR spectroscopy in its differential diagnosis. MagnReson Imaging1995;13:1019–1029.

17. Poptain H, Gupta RK, Roy R, et al. Characterization of intracranial mass lesions with in vivo proton MR spectroscopy. AJNR Am J Neuroradiol 1995;16:1593–1603

18. Grand S, Passaro G, Ziegler A, et al. Necrotic tumor versus brain abscess: importance of amino acids detected at 1H MR spectroscopy—initial results. Radiology1999;213:785–793

19. Gupta RK, Husain N, Kathuria MK, Datta S, Rathore RK, Husain M. Magnetization transfer MR imaging correlation with histopathology in intracranial tuberculomas. ClinRadiol.2001;56:656–63.

20. Gupta RK, Lufkin RB. In Tuberculosis and other non-tuberculous bacterial granulomatous infection. New York: Kluwer Academic/Plenum Publishers; 2001. MR imaging and spectroscopy of central nervous system infection; pp. 95–145

21. Poptani H, Gupta RK, Roy R, Pandey R, Jain VK, Chhabra DK. Characterization of intracranial mass lesions with in vivo proton MR spectroscopy. AJNR Am J Neuroradiol.1995;16:1593–603.

22. Potts DG, Abbott GF, von Sneidern JV. National Cancer Institute study: evaluation of computed tomography in the diagnosis of intracranial neoplasms. III. Metastatic tumors. Radiology1980;136:657–664.

23. Posner JB, Chernik NL. Intracranial metastases from systemic cancer. AdvNeurol1978;19:579–592.

24. Meyer PC, Reah TG. Secondary neoplasms of the central nervous system and meninges. Br J Cancer1953;7:438.

25. Mandybur TI. Intracranial hemorrhage caused by metastatictumors. Neurology1977;27:650–655.

26. Zimmerman RA, Bilaniuk LT. Computed tomography of acute intratumoral hemorrhage. Radiology1980;135:355–359

27. Vieth RG, Odom GL. Intracranial metastases and their neurosurgical treatment. J Neurosurg1965;23:375–383.

28. Kleihues P, Cavenee WK, eds. Pathology and genetics of tumours of the nervous system. Lyon, France: IARC Press,2000.

29. DiMario FJ, Ramsby G, Greenstein R, et al. Neurofibromatosis type I: magnetic resonance imaging findings. J Child Neurol1993;8:32–39.

30. Kornreich L, Blaser S, Schwarz M, et al. Optic pathway glioma: correlation of imaging findings with the presence of neurofibromatosis. Am J Neuroradiol2001;22:1963–1969.

31. Maarouf M, Kuchta J, Miletic H, Ebel H, Hesselmann V, Hilker R, etal. Acute demyelination: diagnostic difficulties and the need for brain biopsy. ActaNeurochir (Wien)2003;145:961-9.

32. Masdeu JC, Quinto C, Olivera C, Tenner M, Leslie D, Visintainer P. Open-ring sign: highly specific for atypical brain demyelination. Neurology 2000;54:1427-33.

33. Schwartz KM, Erickson BJ, Lucchinetti C Pattern of T2 hypointensity associated with ring-enhancing brain lesions can help to differentiate pathology Neuroradiology. 2006Mar;48(3):143-9

34. Vasudev MK, Jayakumar PN, Srikanth SG, Nagarajan K, Mohanty A Quantitative magnetic resonance techniques in the evaluation of intracranial tuberculomasActaRadiol. 2007Mar;48(2):200-6.

35. Kalita J, Prasad S, Maurya PK, Kumar S, Misra UK. MR angiography in tuberculous meningitis ActaRadiol. 2012 Apr1;53(3):324-9

36. Batra A, TripathiRP.Diffusion-weighted magnetic resonance imaging and magnetic resonance spectroscopy in the evaluation of focal cerebral tubercular lesions. ActaRadiol. 2004Oct;45(6):679-88

37. Gupta RK, Husain M, Vatsal DK, Kumar R, Chawla S, Husain N. Comparative evaluation of magnetization transfer MR imaging andin-vivo

proton MR spectroscopy in brain tuberculomas. MagnReson Imaging. 2002 Jun;20(5):375-81

38. SalgadoP,DelBruttoOH,TalamásO,ZentenoMA,Rodríguez-Carbajal J. Intracranial tuberculoma: MR imaging Neuroradiology. 1989;31(4):299-302.
39. Chang KH, Han MH, Roh JK, Kim IO, Han MC, Choi KS, Kim CW Gd-DTPA enhanced MR imaging in intracranial tuberculosis. Neuroradiology. 1990;32(1):19-25.
40. Daoud E, Mezghani S, Fourati H, Ketata H, Guermazi Y, Ayadi K, Dabbeche C, Mnif J, Ben Mahfoudh K, Mnif Z MR imaging features of tuberculosis of the sellar region J Radiol. 2011Jul-Aug;92(7-8):714-21.
41. AmaralL, Maschietto M, Maschietto R, Cury R, Ferreira NF, Mendonça R, Lima SS. Ununsual manifestations of neurocysticercosis in MR imaging: analysis of 172 cases ArqNeuropsiquiatr. 2003 Sep;61(3A):533- 41.
42. Chang KH, Han MH MRI of CNS parasitic diseases. J MagnReson Imaging. 1998 Mar-Apr;8 (2):297-307.
43. HR Martinez,R Rangel- Guerra, G Elizondo, J Gonzalez, LE Todd, J Ancer, and SS Prakash MR Imaging in neurocysticercosis: a study of 56 cases AJNR 1989 ; 10 (5) :1011-1019
44. Haris M, Gupta RK, Singh A, Husain N, Husain M, Pandey CM, Srivastava C, Behari S, Rathore RK. Differentiation of infective from neoplastic brain lesions by dynamic contrast-enhanced MRI Neuroradiology. 2008 Jun;50(6):531-40 Epub 2008 Apr1

45. Savita R Singhal, Smiti Nanda1 and Suresh K SinghalNeurocysticercosis as an important differential of seizures in pregnancy: two case reports Journal of Medical Case Reports 2011,5:206

46. D. Pal , A. Bhattacharyya ,M. Husain ,K.N. Prasad ,C.M. Pandey ,R.K. Gupta In Vivo Proton MR Spectroscopy Evaluation of Pyogenic Brain Abscesses: A Report of 194 Cases AJNR Am J Neuroradiol Feb 2010 31:360–66

47. Mao J, Li J, Chen D, Zhang J, DU YN, Wang YJ, Li X, Wang R, Chen LY, Wang XM Value of MRI in the diagnosis of cerebral abscess caused by Candida albicans in premature infants Zhongguo Dang Dai ErKeZaZhi. 2011Aug;13(8):621-6.

48. G. Luthra,A. Parihar, K. Nath,S. Jaiswal,K.N. Prasad et al Comparative Evaluation of Fungal, Tubercular, and Pyogenic Brain Abscesses with Conventional and Diffusion MR Imaging and Proton MR Spectroscopy AJNR Am J Neuroradiol Aug200728:1332–38

49. Hakyemez B, Ergin N, Uysal S, Işik I, Kiliç E Diffusion-weighted mri in the differentiation of brain abscesses and necrotic tumors TaniGirisimRadyol. 2004 Jun;10(2):110-8.

50. Leuthardt EC, WippoldFJ 2nd, Oswood MC, Rich KM. Diffusion- weighted MR imaging in the preoperative assessment of brain abscesses. Surg Neurol. 2002Dec;58(6):395-402;

51. PingH.Lai,JihT.Ho,WeiL.Chen,ShuS.Hsu,JyhS.Wang,Huay B. Pan and Chien F. Yang Brain Abscess and Necrotic Brain Tumor: Discrimination with Proton MR Spectroscopy and Diffusion-Weighted Imaging AJNR Am J Neuroradiol 23:1369–1377, September2002

52. Tsui EY, Chan JH, Cheung YK, Lai KF, Fong D, Ng SH Evaluation of cerebral abscesses by diffusion-weighted MR imaging and MR spectroscopy; Comput Med Imaging Graph. 2002Sep-Oct;26(5):347-51.

53. Fichten A, Toussaint P, Bourgeois P, Gosset JF, Lejeune JP.Diagnostic problems in brain abscess: 45 cases. Neurochirurgie. 2001 Sep;47(4):413-22

54. Kazuhiro Tsuchiya, SayukiInaoka, Yoshiyuki Mizutani, and Junichi Hachiya Fast Fluid-Attenuated Inversion-Recovery MR of Intracranial Infections AJNR Am J Neuroradiol 18:909–913, May1997

55. Shukla-Dave A, Gupta RK, Roy R, Husain N, Paul L, Venkatesh SK, Rashid MR, Chhabra DK, Husain M Prospective evaluation of in vivo proton MR spectroscopy in differentiation of similar appearing intracranial cystic lesions. MagnReson Imaging. 2001Jan;19(1):103-10.

56. X.Z. Chen X.M. Yin L. Ai Q. Chen S.W. Li J.P. Dai Differentiation between Brain Glioblastoma Multiforme and Solitary Metastasis: Qualitative and Quantitative Analysis Based on Routine MR Imaging AJNR Am J Neuroradiol 10.3174/ajnr.A3106

57. Sanjay K. Singh, Norman E. Leeds, and Lawrence E. Ginsberg MR Imaging of Leptomeningeal Metastases: Comparison of Three Sequences AJNR Am J Neuroradiol 23:817–821, May2002

58. Marius Hartmann, Olav Jansen, Sabine Heiland, Clemens Sommer, Kristin Munkel, and Klaus Sartor Restricted Diffusion within Ring Enhancement Is Not Pathognomonic for Brain Abscess AJNR Am J Neuroradiol 22:1738–1742, October 2001

59. Y.M. Tang,S. Ngai,S. Stuckey The Solitary Enhancing Cerebral Lesion: Can FLAIR Aid the Differentiation between Glioma and Metastasis? AJNR Am J Neuroradiol 27:609 –11

60. C.H. Toh, K.-C. Wei,S.-H. Ng , Y.-L.Wan et al Differentiation of Brain Abscesses from Necrotic Glioblastomas and Cystic Metastatic Brain TumorswithDiffusionTensorImagingAJNRAmJNeuroradiol32:1646 –51

61. Kee-Hyun Chang, In Chan Song, Sung Hyun Kim, Moon Hee Han et al In Vivo Differentiation of Aerobic Brain Abscesses and Necrotic Glioblastomas Multiforme Using Proton MR Spectroscopic Imaging AJNR Am J Neuroradiol29:1511–18

62. P.H. Lai, H.H. Weng C.Y, Chen S.S. Hsu et al(2008) In Vivo Differentiation of Aerobic Brain Abscesses and Necrotic Glioblastomas Multiforme Using Proton MR Spectroscopic Imaging AJNR September 2008 29:1511-1518

63. W. Hollingworth L.S. Medina R.E. Lenkinski D.K. Shibata et al A Systematic Literature Review of Magnetic Resonance Spectroscopy for the Characterization of Brain Tumors AJNR August 2006 27:1404-1411

64. Mishra AM, Gupta RK, Jaggi RS, et al.Role of diffusion-weighted imaging and in vivo proton magnetic resonance spectroscopy in the differential diagnosis of ring-enhancing intracranial cystic mass lesions. J Comput Assist Tomogr 2004;28:540–47

65. Gupta RK, Prakash M, Mishra AM, et al. Role of diffusion weighted imaging in differentiation of intracranial tuberculoma andtuberculous

abscess from cysticercus granulomas—a report of more than 100 lesions. Eur J Radiol2005;55:384–92

66. Tae Kyoung Kim et al Intracranial Tuberculoma: Comparison of MR with Pathologic Findings AJNR16:1903–1908
67. Jayasundar R, Singh VP, Raghunathan P, Jain K, Banerji AK Inflammatory granulomas: evaluation with proton MRS NMR Biomed. 1999May;12(3):139-44.
68. Suss RA, Maravilla KR, Thompson J MR imaging of intracranial cysticercosis: comparison with CT and anatomopathologic features. AJNR Am J Neuroradiol. 1986 Mar-Apr;7(2):235-42..
69. Kumar A, Kaushik S, Tripathi RP, Kaur P, Khushu S. Role of in vivo proton MR spectroscopy in the evaluation of adult brain lesions: Ourpreliminary experience. Neurol India 2003; 51: 474-478.
70. Gupta RK, Pandey R, Khan EM, Mittal P, Gujral RB, Chhabra DK. Intracranial tuberculomas: MRI signal intensity correlation with histopathology and localized proton spectroscopy. Magn Res Imaging 1993; 11: 443-449.
71. Halmes AB, Zimmerman RD ,MorgelloS,Weingarten K, Becker RD, Jennis R , Deck MD . MR Imaging of brain abscesses . AJR 1989 ;152 (5):1073-85

MASTERCHART

Sl No	NAME	AGE	SEX	C/F	LESION SIDE	LESION LOCATION	T1 MORPHOLOGY	T2 MORPHOLOGY	DIFFUSION	MRS	RADIOLOGICAL DIAGNOSIS
1	ADIVEPPA	46y	M	Seizure and headache	Bilateral	TP	Hypointense	Hypo to isointense	Restriction present	Lip /lac peak	Tuberculoma
2	ANNAPURNA	50y	F	Seizures & Vomiting	Midline	F	Hypointense	Hyperintense	Restriction present	Cho & Lip peak	Primary brain tumour
3	BASAMMA	76y	F	Fever , seizures & vomiting,	Left	FTP	Hypointense	Hyperintense	No restriction	Lip/lac peak & decreased NAA	Tuberculoma
4	BHIMANNA	52y	M	Seizures & Vomiting	Right	F & CGR	Hypointense	Isointense	Restriction present	Choline peak & decreased NAA	Primary brain tumour
5	CHANDRAMMA	35y	F	Seizures & Vomiting	Left	F	Isointense	Isointense	Restriction present	Choline peak	Primary brain tumour
6	FATIMA	35y	F	Seizure, & fever	Right	P	Hypointense	Hyperintense	Restriction present	Lip/lac peak & decreased NAA	Tuberculoma
7	KARTIK	14Y	M	Seizures	Left	F	Hypointense	Hyperintense	No restriction	AA, Lip/lac peak & decreased NAA	NCC
8	KASHIMALI	53y	M	Ataxia, Seizures & Vomiting	Midline	F, CGR & CC	Hypointense	Hyperintense	Restriction present	Choline peak & reversal of Ch:Cr ratio	CNS lymphoma
9	LEELABAI	55y	F	Seizures & Weakness	Right	FP	Hypointense	Isointense	No restriction	Choline peak & decreased NAA	Metastasis
10	MAHESH	28y	M	Seizure & headache	Right	T	Hypointense	Isointense	No restriction	Lip /lac peak	Tuberculoma
11	MALLIKARJUN	69y	M	Seizures & vomiiting	Left	PT	Hypointense	Hyperintense	Restriction present	Choline , Lip peak & decreased NAA	Metastasis
12	PARASAPPA	40y	F	Seizures & left sided weakness	Midline	F & CC	Isointense	Hyperintense	Restriction present	Choline peak	Primary brain tumour
13	PARVATI	65y	M	Seizure & weakness	Left	P	Isointense	Hyperintense	No restriction	Choline , Lip peak & decreased NAA	Primary brain tumour
14	PRIYA	20y	M	Seizures	Left	F	Hypointense	Hyperintense	No restriction	AA, Lip/lac peak	NCC
15	S K NIMBAL	52y	M	Seizure, headache & weakness	Left	FT	Isointense	Hyperintense	Restriction present	Choline peak & decreased NAA	Primary brain tumour

16	**SAGAR**	**24y**	**M**	**Seizures**	**Left**	**Thalamocapsular**	**Hypointense**	**Hypointense**	**No restriction**	**Lip/lac peak & decreased NAA**	**Tuberculoma**
17	**SAIFUSAB**	**55y**	**M**	**Fever, headache, Seizures & ataxia**	**Bilateral**	**L-F, R-O & cerebellum**	**Isointense**	**Hyperintense**	**No restriction**	**Lip/lac peak**	**Tuberculoma**
18	**SANGANNA**	**50y**	**M**	**Fever, seizure & ataxia**	**Right**	**CG & PT**	**Hypointense**	**Hyperintense**	**No restriction**	**Lip/lac peak**	**Tuberculoma**
19	**SANGAPPA**	**63y**	**M**	**Seizure & ataxia**	**Right**	**FTP & CC**	**Hypointense**	**Hyperintense**	**Restriction present**	**Cho & Lip/Lac peak**	**Primary brain tumour**
20	**SAROJINI**	**55y**	**F**	**Seizures**	**Left**	**F**	**Hypointense**	**Hyperintense**	**No restriction**	**Cho, Lip/Lac peak & decreased NAA**	**NCC**
21	**SHANTABAI**	**55y**	**F**	**Seizures**	**Bilateral**	**FTP**	**Hypointense**	**Hyperintense**	**Restriction present**	**Choline peak**	**Metastasis**
22	**SHANTAWWA**	**52y**	**F**	**Seizures & ataxia**	**Bilateral**	**FTO & Cerebellum**	**Hypointense**	**Hyperintense**	**Restriction present**	**Cho, Lip/Lac peak & decreased NAA**	**Metastasis**
23	**SHRISHAIL**	**60y**	**M**	**Seizures**	**Midline**	**FP & CC**	**Isointense**	**Hyperintense**	**Restriction present**	**Cho, Lip/Lac peak & decreased NAA**	**Primary brain tumour**
24	**SIDDARTH**	**10 m**	**M**	**Fever, Seizures, vomiting & ataxia**	**Left**	**FTO**	**Hypointense**	**Hyperintense**	**No restriction**	**AA, & Lip/lac peak**	**Abscess**
25	**SUNITHA**	**40y**	**F**	**Seizures, fever & vomiting**	**Bilateral**	**FTPO**	**Hypointense**	**Hyperintense**	**Restriction present**	**Lip/lac peak**	**Tuberculoma**
26	**VILAS**	**30y**	**M**	**Headache, fever & seizures**	**Bilateral**	**FPT**	**Hypointense**	**Hyerintense**	**No restriction**	**Lip/lac peak**	**Tuberculoma**
27	**RAJSHEKHAR**	**52y**	**M**	**Seizures & ataxia**	**Right**	**FP**	**Hypointense**	**Hyperintense**	**Restriction present**	**AA, & Lip/lac peak**	**Abscess**
28	**HANAMANTH**	**35y**	**M**	**Seizures & fever**	**Left**	**FO & cerebellum**	**Hypointense**	**Hyperintense**	**No restriction**	**Lip/lac peak**	**Tuberculoma**
29	**SURESH K**	**40y**	**M**	**Fever, seizures & ataxia**	**Left**	**FP**	**Hypointense**	**Hyperintense**	**No restriction**	**Lip/lac peak**	**Tuberculoma**
30	**SHEKAGOUDA B**	**42y**	**M**	**Headache & seizures**	**Bilateral**	**FP**	**Hypointense**	**Hyperintense**	**No restriction**	**Lip/Lac peak & decreased NAA**	**Tuberculoma**
31	**SWARNIMA**	**46y**	**F**	**Seizures & weakness**	**Right**	**T**	**Hypointense**	**Hyperintense**	**Restriction present**	**AA, Lip/lac peak & decreased NAA**	**NCC**
32	**NEELAKANTHA YYA**	**28y**	**M**	**Seizures & left hemiparesis**	**Bilateral**	**FTP**	**Hypointense**	**Hyperintense**	**Restriction present**	**AA, Lip/lac peak & decreased NAA**	**Abscess**

BLDE (DEEMED TO BE UNIVERSITY) SHRI B.M.PATIL MEDICAL COLLEGE HOSPITAL AND RESEARCH CENTRE, VIJAYAPUR, KARNATAKA.

CASE PROFORMA

1) Name/ Hospital no. :

2) Age/Sex :

3) Relevant history and complaints :

4) MRI Findings (Plain & Contrast) :

5) MR Spectroscopy Findings :

6) Histo-pathological Diagnosis:

CONSENT FORM

I ……. have been explained in the language I understand the procedure to be performed on my self / my ward and the possible risk / adverse affects of contrast media administration, anaesthesia and the procedure . I , the undersigned , give the informed consent with full knowledge of the risks which have been explained to me.

DATE: NAMEOFPATIENT SIGNATURE OF PATIENT

NOTE : In case the patient is unable to give consent a close relative / attender may give the consent.